Inorg. Chem. **2005**, *44*, 1103–1117

Studies Relevant to Catalytic Reduction of Dinitrogen to Ammonia by Molybdenum Triamidoamine Complexes

Dmitry V. Yandulov[†] **and Richard R. Schrock***

Department of Chemistry, Massachusetts Institute of Technology, Cambridge, Massachusetts 02139

Received August 17, 2004

In this paper we explore several issues surrounding the catalytic reduction of dinitrogen by molybdenum compounds that contain the $[(HIPTNCH_2CH_2)_3N]^{3-}$ ligand (where HIPT = 3,5-(2,4,6-i-$Pr_3C_6H_2)_2C_6H_3$). Four additional plausible intermediates in the catalytic dinitrogen reduction have now been crystallographically characterized; they are **Mo**N═NH (**Mo** = [(HIPTNCH$_2$CH$_2$)$_3$N]Mo), [**Mo**═NNH$_2$][BAr′$_4$] (Ar′ = 3,5-(CF$_3$)$_2$C$_6$H$_3$), [**Mo**═NH][BAr′$_4$], and **Mo**(NH$_3$). We also have crystallographically characterized a 2,6-lutidine complex, **Mo**(2,6-Lut)$^+$, which is formed upon treatment of **Mo**H with [2,6-LutH][B(C$_6$F$_5$)$_4$]. We focus on the synthesis of compounds that have not yet been isolated, which include **Mo**═NNH$_2$, **Mo**═NH, and **Mo**(NH$_2$). **Mo**═NNH$_2$, formed by reduction of [**Mo**═NNH$_2$]$^+$, has not been observed. It decomposes to give mixtures that contain two or more of the following: **Mo**N═NH, **Mo**≡N, **Mo**(NH$_3$)$^+$, **Mo**(NH$_3$), and ammonia. **Mo**═NH, which can be prepared by reduction of [**Mo**═NH]$^+$, is stable for long periods in the presence of a small amount of CrCp*$_2$, but in the absence of CrCp*$_2$, and in the presence of **Mo**═NH$^+$ as a catalyst, **Mo**═NH is slowly converted into a mixture of **Mo**≡N and **Mo**(NH$_2$). **Mo**(NH$_2$) can be produced independently by deprotonation of **Mo**(NH$_3$)$^+$ with LiN(SiMe$_3$)$_2$ in THF, but it decomposes to **Mo**≡N upon attempted isolation. Although catalytic reduction of dinitrogen could involve up to 14 intermediates in a "linear" sequence that involves addition of "external" protons and/or electrons, it seems likely now that several of these intermediates, along with ammonia and/or dihydrogen, can be produced in several reactions between intermediates that themselves behave as proton and/or electron sources.

Introduction

Ever since the first dinitrogen complex of a transition metal, $[Ru(NH_3)_5(N_2)]^{2+}$, was prepared in 1965 (by treating ruthenium salts with hydrazine),[1] scientists have been trying to reduce dinitrogen catalytically to ammonia at room temperature and pressure, or to incorporate dinitrogen in order to prepare nitrogen-containing organic compounds catalytically.[2−11] Chatt, who for many years was actively engaged, as was Hidai, in dinitrogen chemistry involving W(0) and Mo(0) phosphine complexes,[2−4,9,11] believed that it should be possible to reduce dinitrogen to ammonia at a single metal center. Chatt was the first to show that up to 2 equiv of ammonia per metal could be formed from a W(0) dinitrogen complex upon addition of protons, the six electrons being provided by tungsten.[2] Unfortunately, no catalytic reduction of dinitrogen to ammonia using phosphine complexes as catalysts was ever achieved, although Pickett and Talarmin demonstrated that a total of 0.73 equiv of ammonia per W could be obtained electrochemically from $W(N_2)_2(dppe)_2$ and tosylic acid in three cycles.[12] However, we have been able to show relatively recently that it is possible to reduce dinitrogen catalytically to ammonia with protons and electrons at a sterically protected single molybdenum center which assumes oxidation states between and including Mo(III) and Mo(VI) during the catalytic process.[13,14] Only one other room-temperature catalytic reduction

* To whom correspondence should be addressed. E-mail: rrs@mit.edu.
† Present address: Department of Chemistry, Stanford University.

(1) Allen, A. D.; Senoff, C. V. *J. Chem. Soc., Chem. Commun.* **1965**, 621.
(2) Chatt, J.; Dilworth, J. R.; Richards, R. L. *Chem. Rev.* **1978**, *78*, 589.
(3) Hidai, M.; Mizobe, Y. *Chem. Rev.* **1995**, *95*, 1115.
(4) Hidai, M. *Coord. Chem. Rev.* **1999**, *185*−*186*, 99.
(5) Fryzuk, M. D.; Johnson, S. A. *Coord. Chem. Rev.* **2000**, *200*−*202*, 379.
(6) Bazhenova, T. A.; Shilov, A. E. *Coord. Chem. Rev.* **1995**, *144*, 69.
(7) Pickett, C. J. *J. Biol. Inorg. Chem.* **1996**, *1*, 601.
(8) Barriere, F. *Coord. Chem. Rev.* **2003**, *236*, 71.
(9) Richards, R. L. *Coord. Chem. Rev.* **1996**, *154*, 83.
(10) Henderson, R. A.; Leigh, G. J.; Pickett, C. J. *Adv. Inorg. Chem. Radiochem.* **1983**, *27*, 197.
(11) Chatt, J.; Leigh, G. J. *Chem. Soc. Rev.* **1972**, *1*, 121.
(12) Pickett, C. J.; Talarmin, J. *Nature* **1985**, *317*, 652.
(13) Yandulov, D. V.; Schrock, R. R. *J. Am. Chem. Soc.* **2002**, *124*, 6252.

10.1021/ic040095w CCC: $30.25
Published on Web 01/20/2005

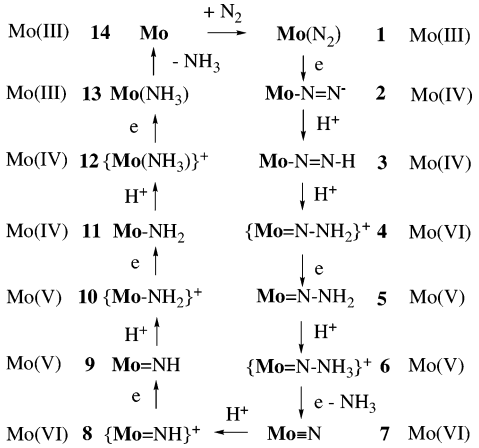

Figure 1. Proposed intermediates in the reduction of dinitrogen at a [HIPTN$_3$N]Mo (**Mo**) center through the stepwise addition of protons and electrons.

of dinitrogen is known.[6,15,16] This system requires and is catalytic in molybdenum, produces mixtures of hydrazine and ammonia (~10:1), and takes place in methanol in the presence of $Mg(OH)_2$ and a strong reducing agent (e.g., Na amalgam). To our knowledge, no details concerning the mechanism of this reaction have been established.

The catalytic system we have developed arose from our interest in the chemistry of Mo complexes that contain a triamidoamine ligand ($[(ArNCH_2CH_2)_3N]^{3-}$ = $[ArN_3N]^{3-}$, Ar = aryl).[17,18] In order to prevent formation of relatively stable and unreactive bimetallic [ArN_3N]Mo−N═N−Mo-[ArN_3N] complexes, maximize steric protection of a monometallic coordination site, and provide increased solubility of compounds in nonpolar solvents, we synthesized species that contain a $[HIPTN_3N]^{3-}$ ligand, where HIPT = 3,5-(2,4,6-i-$Pr_3C_6H_2)_2C_6H_3$ (hexaisopropylterphenyl).[13,19] Starting with **Mo**Cl (**Mo** = [HIPTN$_3$N]Mo) we showed that we could isolate and characterize several intermediates in a hypothetical Chatt-like reduction of dinitrogen, all of which contain the same $[HIPTN_3N]^{3-}$ supporting ligand (Figure 1).[19] These intermediates include paramagnetic **Mo**(N_2) (**1**), diamagnetic $[$**Mo**$(N_2)]^-$ (**2**), diamagnetic **Mo**-N═N−H (**3**), diamagnetic {**Mo**═N−NH_2}{BAr'_4} (**4**; Ar′ = 3,5-$(CF_3)_2C_6H_3$), diamagnetic **Mo**≡N (**7**), diamagnetic {**Mo**═NH}{BAr'_4} (**8**), and paramagnetic {**Mo**(NH_3)}{BAr'_4} (**12**). X-ray studies[19] of **1**, **2** (as two different Mg derivatives), **7**, and **12** all revealed a trigonal pocket in which N_2 or a product of its reduction is protected to a dramatic degree by three HIPT substituents clustered around it. Steric protection of the nitrogen entities within the pocket provided by the bulky HIPT groups is believed to be an important reason several of the most unusual species can be prepared.

Catalytic reduction of dinitrogen was achieved under carefully controlled conditions in heptane using {2,6-lutidinium}{BAr'_4} as the proton source and decamethylchromocene as the electron source.[14] The results of 16 runs using four different Mo derivatives (**1**, **3**, **7**, or **12**) revealed that ~8 equiv of ammonia are formed with an efficiency of 63−66% on the basis of reducing equivalents available. A run employing **Mo**($^{15}N^{15}NH$) under $^{15}N_2$ yielded entirely ^{15}N-labeled ammonia with 66% efficiency. It is assumed at this stage that any equivalents of reducing agent that are not consumed in making ammonia are consumed to form hydrogen, and that no hydrazine is formed. Analogous compounds that contain hexamethylterphenyl or hexa-*tert*-butylterphenyl variations of the $[HIPTN_3N]^{3-}$ ligand are relatively inefficient catalysts for catalytic reduction of dinitrogen to ammonia.[20] The catalytic reaction clearly is extremely finely balanced and might involve as many as all 14 intermediates shown in Figure 1. With the exception of conversion of **6** to **7**, all steps are presumed to be reversible. However, we also believe that at least some of these intermediates themselves are viable electron donors, if not also proton donors, toward other Mo species, and that in solution complex reactions (e.g., disproportionations) might reduce the number of intermediates that must be accessed.

In this paper we structurally characterize several additional plausible intermediates in the catalytic reduction of dinitrogen to ammonia, including **3**, **4**, **8**, and **13**. We also discuss the consequences of attempts to isolate other intermediates shown in Figure 1, electrochemistry with $[Bu_4N][BAr'_4]$ as the electrolyte in fluorobenzene, and a variety of other issues (especially disproportionations) that may prove relevant to catalytic dinitrogen reduction.

Results and Discussion

Conversion of MoN_2 to MoN═NH and the Structure of MoN═NH. We have observed that **Mo**N_2 can be reduced to **Mo**N_2^- with a relatively strong reducing agent such as magnesium, and that **Mo**N_2^- (**2**) can be protonated to yield **Mo**N═NH (**3**).[19] Samples of **3** tend to decompose slowly to yield primarily **Mo**H in a reaction that appears to be catalyzed by traces of acid remaining from the protonation step. However, **3** also appears to decompose in an uncatalyzed reaction. The rate constant for the uncatalyzed decomposition was found to be 2.1×10^{-6} s^{-1} at 61 °C, approximately an order of magnitude slower than typically found for the catalyzed decomposition in which 0.5−1.0% of a $[Et_3NH][BAr'_4]$ impurity is believed to be present. The precise mechanism of each type of decomposition is not known. The tendency for **3** to decompose to **Mo**H led to contamination of **3** by **Mo**H when we attempted to obtain crystals of **3** for X-ray studies. An X-ray study of **3** was considered highly desirable, as a structure search[21] did not yield a crystallographically characterized example of a parent diazenide (NNH) transition metal complex, although there are examples of compounds with related amido-based ligands that contain substituted diazenido ligands, e.g., [(Me_3SiNCH_2-

(14) Yandulov, D. V.; Schrock, R. R. *Science* **2003**, *301*, 76.
(15) Shilov, A. E. *J. Mol. Catal.* **1987**, *41*, 221.
(16) Shilov, A. E. *Russ. Chem. Bull. Int. Ed.* **2003**, *52*, 2555.
(17) Greco, G. E.; Schrock, R. R. *Inorg. Chem.* **2001**, *40*, 3850.
(18) Greco, G. E.; Schrock, R. R. *Inorg. Chem.* **2001**, *40*, 3860.
(19) Yandulov, D. V.; Schrock, R. R.; Rheingold, A. L.; Ceccarelli, C.; Davis, W. M. *Inorg. Chem.* **2003**, *42*, 796.
(20) Ritleng, V.; Yandulov, D. V.; Weare, W. W.; Schrock, R. R.; Hock, A. R.; Davis, W. M. *J. Am. Chem. Soc.* **2004**, *126*, 6150.
(21) Cambridge crystallographic database version 5.25, November 2003.

Table 1. Crystal Data and Structure Refinement for [HIPTN$_3$N]MoN═NH, {[HIPTN$_3$N]Mo═NNH$_2$}[BAr′$_4$], {[HIPTN$_3$N]Mo═NH}[BAr′$_4$], [HIPTN$_3$N]MoNH$_3$, and {[HIPTN$_3$N]Mo(2,6-lutidine)}[B(C$_6$F$_5$)$_4$][a]

	MoN═NH	**Mo**N═NH$_2^+$	**Mo**═NH$^+$	**Mo**NH$_3$	**Mo**(2,6-lutidine)$^+$
empirical formula	$C_{123.5}H_{159}N_6Mo$[b]	$C_{154.5}H_{173}BF_{24}N_6Mo$	$C_{153.5}H_{172}BF_{24}N_5Mo$	$C_{116}H_{162}N_5Mo$	$C_{164.75}H_{183}BF_{20}N_5Mo$
fw	1823.51	2676.74	2649.71	1722.45	2719.91
cryst syst	monoclinic	triclinic	triclinic	monoclinic	monoclinic
space group	$P2_1/n$	$P\bar{1}$	$P\bar{1}$	Cc	$P2_1/n$
a (Å)	18.4395(12)	15.6955(9)	15.6135(16)	16.0506(9)	17.8741(10)
b (Å)	39.343(3)	20.5563(11)	20.226(2)	40.126(2)	30.5416(18)
c (Å)	19.4500(13)	26.1006(15)	26.128(3)	18.0390(10)	28.3608(16)
α (deg)	90	84.9670(10)	84.910(2)	90	90
β (deg)	117.5870(10)	83.6400(10)	84.369(2)	93.61(3)	96.550(18)
γ (deg)	90	82.3940(10)	82.826(2)	90	90
V (Å^3)	12506.2(14)	8272.8(8)	8122.(15)	11594.9(11)	15381.2(15)
Z	4	2	2	4	4
density (calcd; Mg/m^3)	0.968	1.075	1.083	0.987	1.175
abs coeff (mm^{-1})	0.148	0.151	0.153	0.156	0.160
F(000)	3936	2810	2782	3740	5734
cryst size (mm^3)	0.40 × 0.19 × 0.19	0.48 × 0.31 × 0.22	0.20 × 0.20 × 0.08	0.31 × 0.14 × 0.14	0.20 × 0.14 × 0.08
θ range (deg)	1.95−22.50	2.32−25.00	2.14−20.82	1.98−24.69	1.28−21.97
index ranges	$-19 \le h \le 17$	$-18 \le h \le 18$	$-15 \le h \le 15$	$-16 \le h \le 18$	$-18 \le h \le 18$
	$0 \le k \le 42$	$-24 \le k \le 24$	$-20 \le k \le 20$	$0 \le k \le 47$	$0 \le k \le 32$
	$0 \le l \le 20$	$0 \le l \le 30$	$0 \le l \le 26$	$-21 \le l \le 17$	$0 \le l \le 29$
reflns collected	45870	37682	25170	25958	65757
indep reflns [R(int)]	16317 [0.1245]	28305 [0.0551]	16885 [0.0722]	13829 [0.0542]	18771 [0.0734]
completion to θ_{max} (%)	99.9	97.2	99.2	99.8	100
data/restraints/params	16317/1732/1238	28305/3067/1976	16885/2495/1827	13829/75/1137	18771/276/1799
GOF on F^2	1.203	1.052	1.049	1.057	1.036
final R indices [$I > 2\sigma(I)$]	R1 = 0.1376	R1 = 0.0937	R1 = 0.1024	R1 = 0.0638	R1 = 0.0558
	wR2 = 0.3063	wR2 = 0.2459	wR2 = 0.2682	wR2 = 0.1519	wR2 = 0.1608
R indices (all data)	R1 = 0.1843	R1 = 0.1215	R1 = 0.1467	R1 = 0.0883	R1 = 0.0957
	wR2 = 0.3274	wR2 = 0.2662	wR2 = 0.3018	wR2 = 0.1667	wR2 = 0.1852
peak and hole (e Å^{-3})	1.289 and −1.641	1.639 and −0.734	1.628 and −0.796	0.686 and −0.411	0.759 and −0.380

[a] In all cases the temperature (K) = 193(2), the wavelength (Å) = 0.71073, the refinement method was full-matrix least-squares on F^2, and the absorption correction was semiempirical from equivalents. See Supporting Information for the number and identity of solvent molecules included in the empirical formula. [b] This formula was calculated on the basis of a homogeneous crystal consisting of 85% **Mo**N═NH and 15% **Mo**H.

Table 2. Structural Parameters of Mo Intermediates in Catalytic Dinitrogen Reduction[a]

	MoN$_2$[c]	Mo−N═N− [b]	**Mo**N═NH	**Mo**═NNH$_2^+$	**Mo**≡N[c]	**Mo**═NH$^+$	**Mo**(NH$_3$)$^+$ [c]	**Mo**(NH$_3$)
oxidation state/Mo electron count[d]	III/17	IV/18	IV/18	VI/18	VI/18	VI/18	IV/16	III/17
Mo−N$_{amide}$ (av)	1.978	2.030	2.010	1.954	2.003	1.944	1.948	2.003
Mo←N$_{amine}$	2.188(4)	2.241(6)	2.228(7)	2.236(4)	2.395(5)	2.286(6)	2.147(9)	2.205(5)
Mo−N$_\alpha$	1.963(5)	1.863(7)	1.780(9)	1.743(4)	1.652(5)	1.631(7)	2.236(10)	2.170(6)
N$_\alpha$−N$_\beta$	1.061(7)	1.156(8)	1.302(13)	1.304(6)				
Ar(i)/Mo−N−C−C[e]	58.4°	33.6°	28.2°	63.8°	27.5°	64.6°	67.4°	57.1°

[a] Bond lengths (Å) and angles (deg). [b] See ref 19 for the MgBr(THF)$_3$ derivative; the structure is drawn with the negative charge localized on the β nitrogen. [c] See ref 19. [d] Only four of the six amido π electrons are counted, since two π electrons are in a nonbonding ligand MO on the amido nitrogens. Any electron pair on an α nitrogen is also counted toward the total. [e] Average angles between the mean-square planes between the amido nitrogens and the aryl rings attached to each amido nitrogen.

$CH_2)_2NCH_2CH_2NMe_2]Mo(N{=}NSiMe_3)(Me)$[22] or {[(Me$_3$SiNCH$_2CH_2$)$_2NCH_2CH_2NMe_2$]Mo−N═NSiMe$_3$}OTf.[22]

A suitable crystal of "**Mo**N═NH" finally was obtained and a single crystal X-ray study was carried out successfully (Figure 2).[23] Crystal parameters can be found in Table 1 and selected bond distances and angles in Table 2. (A complete list of bond distances and angles can be found in the Supporting Information.) Although most of the structure behaved normally, the nitrogen atoms of the diazenide ligand were subject to excessive thermal motion. The isotropic thermal parameter for N5 could be brought to within a reasonable range of 1.0−1.5 times that of the other nitrogen atoms in the immediate vicinity of Mo by limiting the site occupancy factor of the NNH ligand to between 0.83 and 0.88. We believe that the particular crystal chosen for the

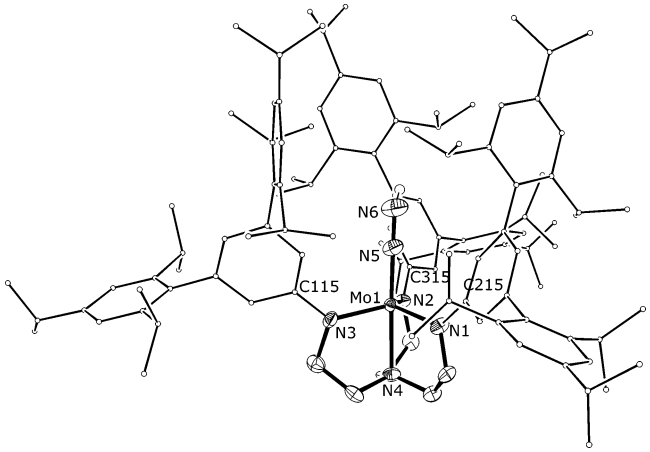

Figure 2. Structure of **Mo**N═NH with hydrogens omitted (except N6H).

(22) O'Donoghue, M. B.; Davis, W. M.; Schrock, R. R. *Inorg. Chem.* **1998**, *37*, 5149.

(23) It has often required months to obtain crystals of compounds that contain the [HIPTN$_3$N]$^{3-}$ ion. Also the crystals often do not yield intense data, and the overall structure quality consequently suffers. We do not expect to be able to solve this inherent limitation. (See also ref 19.)

X-ray study consisted of a mixture of **Mo**N═NH and cocrystallized **Mo**H in the same space group in a way that perfectly overlaps the Mo fragments. By proton NMR we have observed **Mo**H in crystalline **Mo**H═NH samples obtained under conditions analogous to those that produced the crystals for the X-ray study. Therefore, in the final stages of refinement, the atoms of the NNH ligand were assigned site occupancy factors of 0.85; nevertheless, the resultant geometric parameters were within 2σ of those obtained with a full-occupancy model. The diazenide ligand is linear at N_α (Mo−N5−N6 = 179.5(10)°), and the Mo−N5 and N5−N6 bond lengths of 1.780(9) and 1.302(13) Å are consistent with values found (1.789(2) and 1.229(3) Å, respectively) in a related compound of this general type, $[(Me_3SiCH_2CH_2N)_2NCH_2CH_2NMe_2]Mo(N{=}NSiMe_3)(Me)$.[22] It is possible that N_α in the diazenide ligand is not *precisely* trans to N4, since the N5−Mo−N4 angle is 178.0(4)°, although the deviation from 180° is not considered statistically significant enough to be certain. The NNH hydrogen was not located in the difference density map, but was refined in a calculated position, assuming sp^2 hybridization at N6. Presence of the NNH hydrogen in the refinement model did not affect the geometry of the MoNN fragment. It should be noted that $N_\alpha-N_\beta-R$ angles in diazenido compounds vary, e.g., from 132° in $[(Me_3SiNCH_2CH_2)_2NCH_2CH_2NMe_2)]Mo(CH_3)(N_2TMS)$[22] to 170° in $\{[(Me_3SiNCH_2CH_2)_2NCH_2CH_2NMe_2]Mo-N{=}NSiMe_3\}OTf$.[22] Therefore we cannot say where exactly H_β is located. Compound **3** is believed to be the first unambiguous, crystallographically characterized, parent diazenido (M═N−NH) complex, and it is derived from a dinitrogen complex by addition of a proton and an electron.

We have found that it is possible to prepare **3** from **1** using $CoCp_2$ as the reducing agent and [2,6-LutH][BAr′$_4$] as the acid source in C_6D_6. For example, addition of 1.0 equiv of [2,6-LutH][BAr′$_4$] and 2.0 equiv of $CoCp_2$ to **1** resulted in immediate and essentially quantitative conversion of **1** to **3**, according to NMR spectra of reaction mixtures. When 7.0 equiv of [2,6-LutH][BAr′$_4$] and 8.2 equiv of $CoCp_2$ were employed, **Mo**$(NH_3)^+$ (**12**) was the sole observable **Mo**-containing product. No species other than **3** or **12** was observed using quantities of [2,6-LutH][BAr′$_4$] and $CoCp_2$ between the low and high values quoted. We also found that **Mo**≡N could be reduced to **12** in C_6D_6 in the presence of 3.5 equiv of [2,6-LutH][BAr′$_4$] and 4.2 equiv of $CoCp_2$, and confirmed that pure **12** is not reduced rapidly in C_6D_6 by cobaltocene to give **13** or **14**. (See discussion of the reduction of **12** later.) One-electron, one-proton reduction of **Mo**N_2 to **Mo**N═NH takes place with any combination of three acids ([Et_3NH][OTf], [Et_3NH][BAr′$_4$], [2,6-LutH][BAr′$_4$]) and two reductants ($CoCp_2$ and $CrCp^*_2$), and is rapid in all cases. However, the mechanism of this process is still in doubt. In view of the importance of conversion of a dinitrogen complex into a diazenido complex in the Chatt dinitrogen reduction scheme, we will consider this reaction in some detail.

The three mechanisms that we believe are most plausible are shown in Scheme 1. The mechanism that we consider the least likely consists of protonation of the *neutral* dinitrogen complex at N_β, followed by reduction (path A).

Scheme 1. Three Possible Mechanisms for Addition of a Proton and an Electron to MoN_2 To Yield **Mo**−N═NH

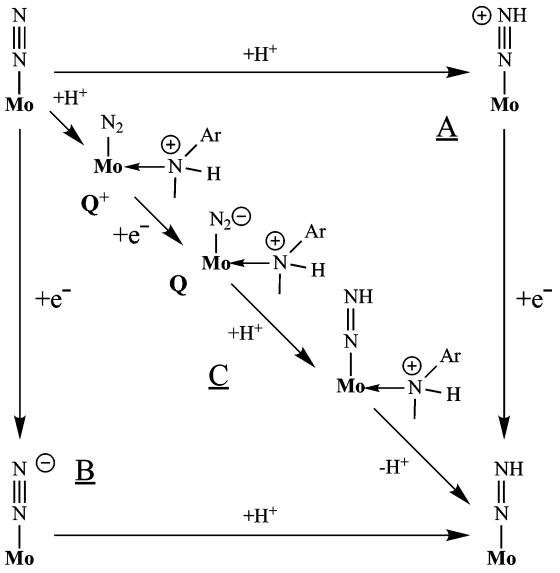

Table 3. Electrochemical Properties of Catalytic Mo Intermediates and Metallocene Reductants[a]

couple	$E^{\circ\prime}$(THF)	$E^{\circ\prime}$(PhF)
Mo$N_2^{+/0}$	−0.42 (I_{pa})[b]	−0.66
Mo$N_2^{0/-}$	−1.81	−2.01
MoN═$NH^{+/0}$		∼0[c]
Mo═$NNH_2^{+/0}$	1.47 (I_{pc})[d]	−1.56 qr[e]
Mo═$NH^{+/0}$	−1.25 qr	−1.38 qr
Mo$(NH_3)^{+/0}$	−1.51	−1.63
$CoCp_2^{+/0}$	−1.33	−1.33
$CrCp^*_2{}^{+/0}$	−1.47	−1.63
$CoCp^*_2{}^{+/0}$	−1.84	−2.01

[a] Formal potentials ($E^{\circ\prime}$, V) measured by cyclic voltammetry in 0.4 M [Bu_4N][PF_6] in THF at 1.6 mm Pt disk, or 0.1 M [Bu_4N][BAr′$_4$] in PhF at 3.0 mm glassy carbon disk at 22 °C and referenced to $FeCp_2^{+/0}$. [b] Anodic peak potential of irreversible oxidation at scan rate of 500 mV/s. [c] Onset of multiple irreversible oxidation waves. [d] Cathodic peak potential of irreversible reduction at scan rate of 50 mV/s. [e] qr = quasireversible.

One reason we believe path A to be unlikely is that we could find no documented, clear-cut example in the literature of protonation of a *neutral* dinitrogen complex to give a cationic M−N═NH species. The second reason is that addition of [2,6-LutH][BAr′$_4$] to **Mo**N_2 yields no evidence that N_β is protonated. Instead, a proton adds to another site. (See below.) Third, we find that protonation of **Mo**N_2 with [$H(OEt_2)_2$][BAr′$_4$] in either C_6D_6 at room temperature or ether at −25 °C followed by warming to room-temperature resulted in complex mixtures of products that contained on the order of 20% **Mo**═NNH_2^+. Attempted electrochemical generation of "[**Mo**N═NH]$^+$" by oxidation of **Mo**N═NH (**3**) was also unsuccessful; oxidation of **3** in PhF with 0.1M [Bu_4N][BAr′$_4$] electrolyte at room temperature was found to be totally irreversible (Table 3) at a scan rate of 500 mV/s.

Addition of 1 equiv of [2,6-LutH][BAr′$_4$] to **Mo**N_2 in C_6D_6 reveals no change by both ^{1}H NMR and IR over a period of 24 h. However, an IR spectrum of a mixture of 1 equiv of **Mo**N_2 and 2 equiv of [2,6-LutH][BAr′$_4$] in fluorobenzene reveals that ∼30% of a new species is formed with a ν(N−N) absorption shifted by 67 cm^{-1} to higher energy from

that for **Mo**N_2, consistent with decreased back-bonding into the dinitrogen ligand. No new *low*-energy absorption is observed, as would be expected if N_β of the dinitrogen ligand were protonated. Either the acid has hydrogen-bonded to a Brønsted basic site in **Mo**N_2, and the complex has acquired a partial positive charge, or a proton has actually transferred to that basic site to give a cationic species. The most likely Brønsted basic site we believe to be an amido nitrogen. (One linear combination of p orbitals on the amido nitrogens that is centered on the three amido nitrogens contains two electrons.) However, we cannot dismiss the metal itself or the amine donor as the Brønsted basic site, if we assume that the amine can dissociate from the metal and invert configuration at nitrogen. Let us assume that a proton actually transfers from lutidine to an amido nitrogen atom, as shown in Scheme 1 (path C). The resulting cation should then be much more easily reduced. For example, Sellman has shown that protonation of thiolates in iron carbonyl thiolate complexes can result in a high-energy shift of ν(C−O) by 40 cm^{-1} and a positive shift of the reduction potential by 600 mV.[24] If the electron still adds most readily to the Mo-dinitrogen unit in $\mathbf{Q}^+$, a zwitterion, **Q**, is produced which should be prone to protonation at N_β as a consequence of the charge being localized largely on N_β. Deprotonation of the amine to reform the amide would complete the formation of **Mo**N═NH. This process could be called a proton-catalyzed reductive protonation. However, in the absence of additional characterization of the proposed intermediate or intermediates, mechanism C remains tentative. Furthermore, in view of the ability of 2,6-lutidine to bind to a [HIPTN$_3$N]-Mo^+ center (vide infra), we should also consider the possibility that the protonated amide arm in $\mathbf{Q}^+$ is actually displaced by 2,6-lutidine before an electron is added to the dinitrogen ligand.

We believe that mechanism B is the most likely of the three, i.e., **Mo**N_2 is first reduced (probably incompletely) to **2**, which is then protonated. Electrochemical studies reveal that reduction of **Mo**N_2 is fully reversible in both THF (0.4 M [Bu_4N][PF_6]) and PhF (0.1 M [Bu_4N][BAr′$_4$]), with redox waves being observed at −1.81 and −2.01 V, respectively, versus $FeCp_2^{+/0}$ (Table 3). Isolated [Bu_4N][**Mo**N_2][19] shows an identical CV in THF in the reverse scan direction. The 120−200 mV negative shifts observed on going from THF (0.4 M [Bu_4N][PF_6]) to PhF (0.1 M [Bu_4N][BAr′$_4$]) electrolyte for all potentials measurable in both solvents in Table 3, except for $CoCp_2^{+/0}$, reflect a reduction of the strength of ion-pairing interactions that favor formation of positively charged species, relative to that affecting the reference couple, $FeCp_2^{+/0}$.[25,26] Data in fluorobenzene with [Bu_4N]-[BAr′$_4$] as the electrolyte data are thus better suited for estimating equilibrium constants from redox potentials. However, electrode potentials of reactions taking place in heptane (the solvent employed in catalytic dinitrogen reduction) are likely to be altered significantly by precipitation of the complementary redox forms from solution altogether, which can drive otherwise unfavorable reactions forward. For example, the electrochemical potential of [HTBTN$_3$N]-$Mo(NH_3)^{+/0}$ (HTBT = hexa-*tert*-butylterphenyl) is 140 mV negative of that for $CrCp^*_2{}^{+/0}$ (both measured in THF with [Bu_4N][PF_6] electrolyte), yet reduction of {[HTBTN$_3$N]Mo-(NH_3)}[BAr′$_4$] with 2 equiv of $CrCp^*_2$ in C_6D_6 proceeds nearly to equimolar equilibrium.[20] This demonstrates that precipitation of [$CrCp^*_2$][BAr′$_4$] from C_6D_6 can lower the effective potential difference by up to 140 mV from what it is in THF ([Bu_4N][PF_6]). This effect is likely to be much more pronounced in heptane, the solvent used in catalytic runs. The effect of ion pairing and precipitation of products is likely to be similar or greater than it is in PhF with [Bu_4N]-[BAr′$_4$] electrolyte and thus make the chemical reductants that we have chosen effectively stronger in heptane. It should also be noted that catalytic reduction of dinitrogen is successful with cobaltocene as a reducing agent (3.6 equiv of ammonia with **Mo**≡N as the catalyst), which is a weaker reducing agent than $CrCp^*_2$ in THF by 140 mV.[20]

Protonation of [**Mo**N_2]$^-$ is facile, apparently proceeding within the time of mixing even with [Et_3NH][OTf] in ether. (The pK_a of [Et_3NH]Cl in water is 10.81,[27] while the pK_a of [2,6-LutH]Cl in water is 6.75.[28]) The pK_α of **Mo**N═NH appears to be approximately the same as that of $DBUH^+$ in THF,[29] since **Mo**N═NH can be deprotonated to a considerable degree by DBU in THF. Interestingly, an IR spectrum of this equilibrium mixture shows that ν(N−N) in [DBUH]-[**Mo**N_2] is 22 cm^{-1} *higher* in energy than ν(N−N) in [Bu_4N]-[**Mo**N_2]. We would expect [**Mo**N_2]$^-$ to be protonated readily by [2,6-LutH][BAr′$_4$] in the catalytic dinitrogen reduction runs, although the approximate difference of 4 pK_a units between Et_3NH^+ and 2,6-$LutH^+$ in water can only serve as a guideline for acid/base behavior in nonpolar solvents.

In summary, mechanism B at this stage appears to us to be the most viable pathway for conversion of **Mo**N_2 to **Mo**N═NH, as long as electron transfer to **Mo**N_2 to yield MoN_2^- and protonation of MoN_2^- are both fast. However, it is also true that neither path A nor path C can be ruled out at this point in the absence of quantitative kinetic data and appropriate thermodynamic information.

X-ray Structure and Reduction of Mo═NNH_2^+. We have reported previously that protonation of **Mo**−N═NH with [$H(OEt_2)_2$][BAr′$_4$] in C_6D_6 affords [**Mo**═N−NH_2]-[BAr′$_4$] nearly quantitatively in 2 h at 22 °C (according to ^{1}H NMR studies).[19] [**Mo**═N−NH_2][BAr′$_4$] was isolated in 68% yield from the analogous reaction in ether (1.5 h) and fully characterized. However, protonation of **Mo**N═NH with 1 equiv of [2,6-LutH][BAr′$_4$] in C_6D_6 yields a 44:56 equilibrium mixture of **Mo**N═NH and **Mo**═NNH_2^+ (K_{eq} = 1.6) after 15 min at 22 °C. In the ^{1}H NMR spectrum resonances for both **Mo**N═NH and **Mo**═NNH_2^+ can be observed and they are broadened only slightly, which

(24) Sellmann, D.; Sutter, J. *Acc. Chem. Res.* **1997**, *30*, 460.
(25) Astruc, D. In *Electron Transfer in Chemistry*; Balzani, V., Ed.; Wiley-VCH: New York, 2001; Vol. 2, Chapter 4.
(26) LeSuer, R. J.; Geiger, W. E. *Angew. Chem., Int. Ed.* **2000**, *39*, 248.
(27) Ralph, E. K.; Grunwald, E. *J. Am. Chem. Soc.* **1967**, *89*, 2963.
(28) Brown, H. C.; Mihm, X. R. *J. Am. Chem. Soc.* **1955**, *77*, 1723.
(29) Rodima, T.; Kaljurand, I.; Pihl, A.; Mäemets, V.; Leito, I.; Koppel, I. A. *J. Org. Chem.* **2002**, *67*, 1873.

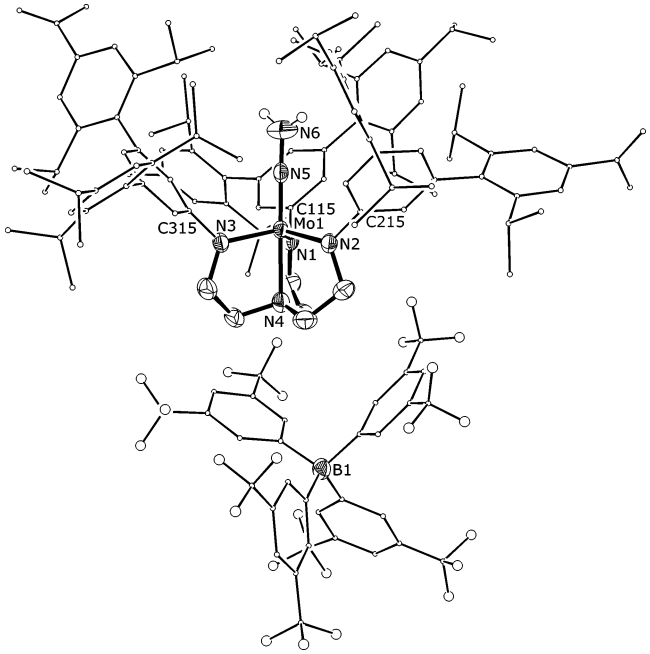

Figure 3. Structure of [**Mo**=NNH_2][BAr'_4] with hydrogens omitted (except $N6H_2$).

suggests that the proton exchange rate between **Mo**N=NH and **Mo**=NNH_2^+ is not fast on the NMR time scale under these conditions. (Proton transfer almost certainly could not take place directly in a reaction that is bimolecular in Mo, but would require some base, e.g., lutidine, as the proton carrier.) Conversion of **Mo**N_2 into **Mo**N=NH in the presence of limited acid and reductant (vide supra) stops at the **Mo**N=NH stage, most likely because the rate of conversion of **Mo**N_2 into **Mo**N=NH is rapid, and the reaction between **Mo**N=NH and **Mo**=NNH_2^+ (in the presence of [2,6-LutH][BAr'_4] and 2,6-lutidine) is readily reversible. Yet in the presence of excess acid and reductant no intermediates between **Mo**N=NH and **Mo**$(NH_3)^+$ are observed (vide supra). The consequences of reduction of **Mo**=NNH_2^+ are described below.

A single-crystal X-ray study of [**Mo**=NNH_2][BAr'_4] has been successful (Figure 3; Tables 1 and 2). The Mo−N5−N6 fragment is possibly bent slightly at N5 (Mo−N5−N6 = 175.4(4)°) toward one amide nitrogen (N2). Out of six possible orientations of an idealized planar sp^2-hybridized $N_\beta H_2$ unit that were examined (three eclipsing Mo−N(amide) bonds and another set of three obtained by a 90°-rotation around $N_\alpha-N_\beta$, the orientation in which the Mo−N2 bond was eclipsed had difference electron density peaks close to both idealized hydrogen positions. Thus, the structure of [**Mo**=NNH_2][BAr'_4] appears to be ordered and is slightly distorted from an ideal trigonal-bipyramidal geometry that consists of bending of the NNH_2 unit in the plane of the NH_2 group toward one amide nitrogen, concomitant with a slight shortening of the respective Mo−N_{amide} bond (Mo−N2 = 1.953(3)° while Mo−N1 = 1.961(3)° and Mo−N3 = 1.949(3)°). The Mo−N5 and N5−N6 bond lengths of 1.743(4) and 1.304(6) Å, respectively, compare well with the values of 1.747(10) and 1.334(13) Å in {[$N(CH_2CH_2NSiMe_3)_2(CH_2CH_2NCH_3)$]Mo=N−$NMe_2$}OTf,[22] as well as 1.762(12) and 1.333(24) Å in [$(dppe)_2$(F)Mo=NNH_2][BF_4].[30] Protonation of N_β in **Mo**N=NH shortens Mo−N5 and lengthens N5−N6 in the product (Table 2), as one would expect from the dominant resonance structures for each (Figure 1).

Table 4. The Results of Chemical Reductions of **Mo**=NNH_2^+[a]

entry	reductant	**Mo**N=NH	**Mo**≡N	**Mo**$(NH_3)^+$	**Mo**(NH_3)	efficiency, %[b]
1	2 $CoCp_2$	0.83	0	0.17		85
2	1.2 $CrCp^*_2$	0.88	0.06		0.06	42
3	2 $CrCp^*_2$	0.78	0.14		0.08	68
4	4 $CrCp^*_2$[c]	0.63	0.37		0	74
5	2 $CoCp^*_2$[d]	0.55	0.45		0	90

[a] Determined by integration of ^{1}H NMR spectra in C_6D_6 after 10−30 min of mixing the reagents. These spectra also showed complete conversion of **Mo**=NNH_2^+. [b] **Mo**=NNH_2^+ consumed in reactions 4 and 5 (Scheme 2) out of the total amount. [c] Carried out in the presence of 4 equiv of BPh_3. [d] This reaction also yields ∼7% of **Mo**N_2 and 0.39 equiv of NH_3.

Treatment of **Mo**=NNH_2^+ with three different metallocenes ($CoCp_2$, $CrCp^*_2$, or $CoCp^*_2$) in C_6D_6 results in complete consumption of **Mo**=NNH_2^+ at room temperature over a period of 10 min. (Several such experiments are listed in Table 4.) However, resonances consistent with the product that one would expect from one-electron reduction of **Mo**=NNH_2^+, namely **Mo**=NNH_2, were not observed in ^{1}H NMR spectra. Instead mixtures are observed that can be attributed to two competing processes: (i) disproportionation of **Mo**=NNH_2 into **Mo**N=NH and complexes in which dinitrogen is further reduced (i.e., **Mo**≡N, **Mo**$(NH_3)^+$, or **Mo**(NH_3)), and (ii) a net reduction of the acidic proton of **Mo**=NNH_2^+ by the reducing agent. For example, treatment of [**Mo**=NNH_2][BAr'_4] with 2 equiv of $CoCp^*_2$ in C_6D_6 immediately produced a mixture of **Mo**N=NH (0.55) and **Mo**≡N (0.45), along with a yellow precipitate of [$CoCp^*_2$][BAr'_4] (entry 5, Table 4). Indophenol analysis of the volatiles collected from the reaction mixture by vacuum transfer after an additional 26 h revealed that 0.39 equiv of NH_3 had been formed. Therefore, [**Mo**=NNH_2][BAr'_4] and $CoCp^*_2$ appear to react predominantly according to the stoichiometries shown in eq 4 of Scheme 2, which is the sum of elementary steps shown in eqs 1−3. The sequence begins with a one-electron reduction of **Mo**=NNH_2^+ to give "**Mo**=NNH_2" (eq 1), a Mo(V) 17 electron species. "**Mo**=NNH_2" is then protonated by **Mo**=NNH_2^+ to yield **Mo**N=NH, **Mo**≡N, and ammonia, as shown in eqs 2 and 3. The short-lived nature of **Mo**=NNH_2 can be attributed to a combination of a high

Scheme 2. Sequence of Reactions Proposed To Take Place upon Reduction of [**Mo**=NNH_2][BAr'_4][a]

$$\textbf{Mo}{=}NNH_2^+ + \underline{e} \longrightarrow \text{"}\textbf{Mo}{=}NNH_2\text{"} \quad (1)$$

$$\textbf{Mo}{=}NNH_2^+ + \text{"}\textbf{Mo}{=}NNH_2\text{"} \longrightarrow \textbf{Mo}\text{-}N{=}NH + \text{"}\textbf{Mo}{=}NNH_3^+\text{"} \quad (2)$$

$$\text{"}\textbf{Mo}{=}NNH_3^+\text{"} + \underline{e} \longrightarrow \textbf{Mo}{\equiv}N + NH_3 \quad (3)$$

$$2\ \textbf{Mo}{=}NNH_2^+ + 2\ \underline{e} \longrightarrow \textbf{Mo}\text{-}N{=}NH + \textbf{Mo}{\equiv}N + NH_3 \quad (4)$$

$$5\ \textbf{Mo}{=}NNH_2^+ + 4\ \underline{e} \longrightarrow 4\ \textbf{Mo}\text{-}N{=}NH + \textbf{Mo}(NH_3)^+ + NH_3 \quad (5)$$

$$\textbf{Mo}{=}NNH_2^+ + \underline{e} \longrightarrow \textbf{Mo}\text{-}N{=}NH + 0.5\ H_2 \quad (6)$$

[a] $\underline{e}$ = redundant.

(30) Hidai, M.; Kodama, T.; Sato, M.; Harakawa, M.; Uchida, Y. *Inorg. Chem.* **1976**, *15*, 2694.

Brønsted basicity of N_β in combination with the fact that **Mo**=NNH_3^+ (eq 2) is *irreversibly* reduced to yield **Mo**≡N and ammonia (eq 3). The 17 electron Mo(V) species, "**Mo**=NNH_3^+", is likely to be reduced relatively easily by $CoCp^*_2$, or by a variety of other reducing agents in a typical catalytic reduction.

While thermodynamics may favor steps 2 and 3 strongly, we are puzzled by the apparently facile kinetics of step 2 in C_6D_6, since the extensive steric protection of the apical **Mo** pocket should exclude proton transfer from Mo=NNH_2^+ to Mo=NNH_2 that is bimolecular in Mo. Reduction of **Mo**=NNH_2^+ with weaker reductants, $CrCp^*_2$ or $CoCp_2$, in C_6D_6 results in qualitatively similar decompositions of "**Mo**=NNH_2", although the extent of nitrogen reduction is considerably greater, reaching the **Mo**$(NH_3)^+$ or **Mo**(NH_3) stage (Table 4, entries 1−3). Formation of ammonia complexes in entries 1−3 of Table 4 requires multiple proton-transfers to the intermediate **Mo**≡N, whose Brønsted-basic site is arguably more sterically hindered than N_β of "**Mo**=NNH_2". Therefore we suspect that proton-transfer steps in the absence of a base such as 2,6-lutidine are mediated by an adventitious base, possibly H_3[HIPTN_3N], which is formed in trace quantities in all reactions in Table 4. An attempt to exclude proton-transfer reactivity completely, i.e., by scavenging adventitious base with BPh_3 (Table 4, entry 4), did not change the overall result measurably. It should be noted that amido nitrogens in the ligand can also be protonated (e.g., to yield $\mathbf{Q}^+$ in Scheme 1), and if such a "protonated arm" were to dissociate from the metal, the resulting amine nitrogen could also function as a Brønsted base.

Reductions of **Mo**=NNH_2^+ with $CrCp^*_2$ or $CoCp_2$ reveal substantial deviations of the observed ratios of **Mo** products from the stoichiometries in eqs 4 and 5 and suggest that a competing process (eq 6) effectively raises the relative proportion of **Mo**-N=NH in the product mixture. (The stoichiometries of the processes shown in eqs 4 and 5 are independent of the particular sequence of reactions involved, but are determined solely by the stages of dinitrogen reduction in terms of the limiting reagent (protons) that characterize the complexes in question, i.e., **Mo**N=NH ($1H^+$), **Mo**=NNH_2^+ ($2H^+$), **Mo**≡N ($3H^+$), **Mo**$(NH_3)^+$ ($6H^+$), and **Mo**(NH_3) ($6H^+$).) Free molecular hydrogen was observed by proton NMR in the reaction involving $CoCp_2$ (entry 1). The efficiency of $CrCp^*_2$ reductions (the amount of **Mo**=NNH_2^+ undergoing the reactions shown in eqs 4 and 5 out of the total amount consumed), was found to increase with the amount of reducing agent present. If the reaction shown in eq 6 involved a direct proton-transfer from **Mo**=NNH_2^+ to $CrCp^*_2$, its fraction would not depend on the initial concentration of reductant, since its rate increase would parallel that of the productive reaction shown in eq 1. Instead, the observed increase in efficiency suggests that proton transfer to the added reductant is rate-limited by deprotonation of **Mo**=NNH_2^+ by base, thus reinforcing the suspicion that adventitious base is involved in other proton-transfer steps. It is important to point out that the net process shown in eq 4 requires only a catalytic amount of **Mo**=NNH_2^+, possibly in a redox equilibrium with "**Mo**=NNH_2" (eq 1), and therefore it may be impossible to avoid, at least at room temperature.

Electrochemical reduction of **Mo**=NNH_2^+ is completely irreversible in THF at all scan rates employed. However, use of an electrolyte with negligible Brønsted-basic characteristics (0.1M $[Bu_4N][BAr'_4]$ in PhF) allowed us to observe a quasireversible reduction process at −1.56 V at scan rates as slow as 100 mV/s. Although the peak current ratios I_{pc}/I_{pa} measured for the reduction process in PhF were under 1.3, the cyclic voltammograms were notably asymmetric, with the cathodic wave being considerably broader than the anodic wave. These results suggest that the processes shown in eqs 4 and 5 take place following initial one-electron reduction (eq 1). Proton transfer takes place much faster in THF, so the anodic wave cannot be observed at all. Comparison of the approximate, quasireversible **Mo**=$NNH_2^{+/0}$ potential with those of metallocene reductants (Table 3) shows that while one-electron reduction of **Mo**=NNH_2^+ is possible by both $CrCp^*_2$ and $CoCp^*_2$, even without the added driving force that results from precipitation of $[MCp^*_2][BAr'_4]$ in hydrocarbon solvents, precipitation of $[MCp^*_2][BAr'_4]$ and/or the reactions shown in eqs 4 and 5 allow reduction with $CoCp_2$ also to take place readily.

In summary, the results presented so far suggest that **Mo**=NNH_2^+ is reduced by one electron to yield "**Mo**=NNH_2", which is transformed into products in which nitrogen is further reduced. Although the nitride **Mo**≡N is a plausible and catalytically competent intermediate accessible under catalytic conditions, the actual mechanism of its formation, and the precise nature of "**Mo**=NNH_3^+" remain to be elucidated. However, it should be noted that both ammonia and dihydrogen can be formed.

Protonation of Mo≡N, X-ray Structure of Mo=NH$^+$, Electrochemistry, and Reduction Studies. We previously reported that **Mo**≡N can be protonated with $[H(OEt_2)_2][BAr'_4]$ in ether to yield [**Mo**=NH][BAr'_4] in high yield.[19] However, protonation of **Mo**≡N with 1.1 equiv of [2,6-LutH][BAr'_4] in C_6D_6 gives a 75:25 mixture of **Mo**≡N and **Mo**=NH^+ after 15 min at room temperature; this mixture remains unchanged after 20 h. Protonation of **Mo**≡N to yield **Mo**=NH^+ is therefore a logical and important step in catalytic dinitrogen reduction.

The structure of [**Mo**=NH][BAr'_4] is shown in Figure 4. The Mo−N5 bond length of 1.631(7) Å is statistically the same as what it is in **Mo**≡N (1.652(5) Å; Table 2). The main structural consequence of protonation appears to be a substantial shortening of the $Mo-N_{amine}$ bond (Mo−N4) by 0.11 Å, consistent with a weakening of the trans-influence of the apical ligand upon conversion of **Mo**≡N into **Mo**=NH^+.

Reaction of **Mo**=NH^+ with 2.2 equiv of $CrCp^*_2$ in C_6D_6 instantly and quantitatively yields a paramagnetic, yellow-brown product whose ^{1}H NMR spectrum features a relatively sharp peak at −5.7 ppm and a very broad resonance at +32 ppm. The product is tentatively assigned as the neutral imido species "**Mo**=NH" (**9** in Figure 1). The related, structurally characterized [Me_3SiN_3N]Mo=$NSiMe_3$ also shows a paramagnetically shifted ^{1}H NMR backbone resonance at −4.5

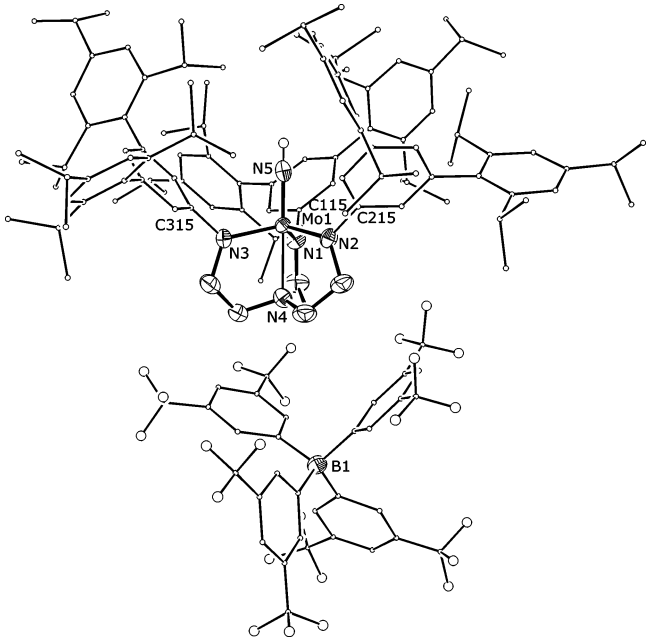

Figure 4. Structure of [**Mo**═NH][BAr′$_4$] with hydrogens omitted (except N5H).

ppm,[31] although this compound is deep blue. "**Mo**═NH" is stable in solution for a week in the presence of at least a small amount of $CrCp^*_2$, although its decomposition (vide infra) upon attempted isolation could not be avoided.

Although "**Mo**═NH" and "**Mo**═NNH_2" are both Mo(V) species, "**Mo**═NH" is considerably more stable than "**Mo**═NNH_2", to the extent that it can be generated in solution and stored for a period of time at room temperature, as long as a small amount of $CrCp^*_2$ is present. In the absence of $CrCp^*_2$, and in the presence of **Mo**═NH^+ as a catalyst, "**Mo**═NH" is slowly converted into a mixture of **Mo**≡N and "**Mo**(NH_2)" (vide infra) via the processes proposed in Scheme 3. Thus, when a substoichiometric amount of $CrCp^*_2$

Scheme 3. Sequence of Reactions Proposed To Take Place upon Reduction of [**Mo**═NH][BAr′$_4$]

$$\mathbf{Mo}(NH)^+ + \underline{e} \longrightarrow \text{"}\mathbf{Mo}(NH)\text{"} \quad (7)$$

$$\mathbf{Mo}(NH)^+ + \text{"}\mathbf{Mo}(NH)\text{"} \longrightarrow \mathbf{Mo}{\equiv}N + \text{"}\mathbf{Mo}(NH_2)^+\text{"} \quad (8)$$

$$\text{"}\mathbf{Mo}(NH_2)^+\text{"} + \text{"}\mathbf{Mo}(NH)\text{"} \longrightarrow \text{"}\mathbf{Mo}(NH_2)\text{"} + \mathbf{Mo}(NH)^+ \quad (9)$$

$$\mathbf{Mo}(NH)^+ + \text{"}\mathbf{Mo}(NH_2)\text{"} \longrightarrow \mathbf{Mo}{\equiv}N + \mathbf{Mo}(NH_3)^+ \quad (10)$$

$$3\ \mathbf{Mo}(NH)^+ + 2\ \underline{e} \longrightarrow 2\ \mathbf{Mo}{\equiv}N + \mathbf{Mo}(NH_3)^+ \quad (11)$$

(~0.6 equiv) was used to reduce **Mo**═NH^+ in C_6D_6, the initially formed "**Mo**═NH" smoothly decayed over a period of hours to form **Mo**≡N and "**Mo**(NH_2)" (vide infra), according to proton NMR spectra of the reaction mixtures. Resonances for "**Mo**(NH_2)" grew in and then disappeared over a period of 9 h, resulting in a final mixture of **Mo**≡N and **Mo**$(NH_3)^+$ (except for residual **Mo**═NH^+), the overall stoichiometry being that shown in eq 11 (Scheme 3).

By analogy with the behavior of "**Mo**═NNH_2", we rationalize the observed transformation shown in eq 11 in terms of the sequence of elementary proton- and electron-transfer steps of eqs 7−10. (Equation 11 = 2 × eq 7 + eq 8 + eq 9 + eq 10.) Although eqs 8 and 9 imply that transformation of "**Mo**═NH" to "**Mo**(NH_2)" proceeds via protonation followed by reduction, an alternative sequence of elementary steps cannot be ruled out. Since the terminal reductant ($CrCp^*_2$) is the limiting reagent in the reaction with **Mo**═NH^+, consumption of "**Mo**═NH" is now "catalyzed" by **Mo**═NH^+, which is consumed and regenerated in eqs 8 and 9, respectively. Notably, such catalysis is also possible when a weaker reductant, $CoCp_2$, is used to generate "**Mo**═NH", even in a two-fold excess: "**Mo**═NH" formed by reduction of **Mo**═NH^+ with 2 equiv of $CoCp_2$ fully decayed in the reaction mixture containing the byproduct [$CoCp_2$][BAr′$_4$] after a period of 21 h into a mixture of analogous disproportionation products. Apparently the initial reduction shown in eq 7 is sufficiently reversible with $CoCp_2$ that an unobserved amount of **Mo**═NH^+ can "catalyze" the conversion of "**Mo**═NH" into **Mo**≡N and **Mo**$(NH_3)^+$.

Compared to the marginal stability of "**Mo**═NNH_2", the greater stability of "**Mo**═NH" may reflect a smaller thermodynamic driving force and/or be the result of slower proton-transfer kinetics (since N_α sites are more sterically congested than N_β sites); as stated before, free ligand (in trace quantities) is believed to be a competent base in circumstances where 2,6-lutidine is not present. The improved kinetic stability of "**Mo**═NH" makes electrochemical reduction of the cationic precursor **Mo**═NH^+ quasireversible in THF (at −1.25 V) as well as in PhF (at −1.38 V; Table 3), although the CVs in PhF still manifest some degree of irreversibility in the form of asymmetric line shapes. The potentials in PhF show that reduction of **Mo**═NH^+ is spontaneous with $CrCp^*_2$ under catalytic conditions, even without the added driving force stemming from precipitation of [$CrCp^*_2$][BAr′$_4$], and support the partial reversibility of the chemical reduction with $CoCp_2$ (vide supra).

Intermediate "**Mo**(NH_2)" can be produced independently by deprotonation of **Mo**$(NH_3)^+$ with $LiN(SiMe_3)_2$ in THF. **Mo**$(NH_3)^+$ is not deprotonated by Et_3N. The ^1H NMR spectrum of "**Mo**(NH_2)", which features methylene backbone resonances at −3.0 and −40.1 ppm, is suggestive of a ground-state high-spin d^2 Mo configuration, or a dynamic high-spin/low-spin equilibrium, which has been identified in the related compound, [RN_3N]$MoNMe_2$ (R = Me_3Si, C_6F_5).[31] The reaction between **Mo**$(NH_3)^+$ and $LiN(SiMe_3)_2$ also produces small and variable amounts of **Mo**N_2 and **Mo**(NH_3). Attempted isolation of "**Mo**(NH_2)" led to the formation of **Mo**≡N. The tendency for "**Mo**(NH_2)" to decompose, along with difficulties in obtaining crystals of this important intermediate, have hampered our attempts to fully characterize it.

In summary, the above results support the proposal that acid and reductant in the catalytic process effect sequential protonation and reduction of intermediate **Mo**≡N to produce metastable "**Mo**═NH". In the presence of **Mo**═NH^+ alone, "**Mo**═NH" is slowly converted into **Mo**≡N and "**Mo**(NH_2)". Although the mechanism of conversion of "**Mo**═NH" into "**Mo**(NH_2)" is not known, this process suggests that acid/

(31) Mösch-Zanetti, N. C.; Schrock, R. R.; Davis, W. M.; Wanninger, K.; Seidel, S. W.; O'Donoghue, M. B. *J. Am. Chem. Soc.* **1997**, *119*, 11037.

base and redox properties of **Mo**=NH$^+$ and "**Mo**=NH" are sufficient for this transformation to proceed to completion and therefore makes "**Mo**(NH_2)" a viable intermediate in the catalytic dinitrogen reduction, in which it is proposed to be protonated to give **Mo**(NH_3)$^+$. Of course **Mo**=NH also can be protonated by lutidinium to give **Mo**(NH_2)$^+$, which can be reduced further by a metallocene reductant to give **Mo**(NH_2), as shown in Figure 1. The relative rates of these competing reactions are not known at this stage.

Reduction of Mo(NH_3)$^+$, Structure of Mo(NH_3), and Exchange of NH_3 for N_2. A ^{1}H NMR spectrum of the catalytic reaction mixture at the end of a catalytic reduction run reveals **Mo**(NH_3)$^+$ to be the only molybdenum species present in any significant amount. The proposed catalytic cycle is "closed" upon one-electron reduction of **Mo**(NH_3)$^+$ to **Mo**(NH_3), followed by exchange of ammonia in **Mo**(NH_3) with dissolved N_2 to yield **Mo**(N_2). Although replacement of ammonia by dinitrogen in dinitrogen reduction schemes has been postulated for decades, upon reflection it is difficult to imagine two η^1 ligands that are more different in how they bind to the same site in a Mo(III) complex. The mechanism, equilibrium, and rate of conversion of **Mo**(NH_3) to **Mo**(N_2) therefore are of great importance.

An equilibrium mixture of **Mo**(NH_3) and **Mo**N_2 is generated upon treating **Mo**N_2 with ammonia or upon reduction of **Mo**(NH_3)$^+$ with $CrCp^*_2$ in C_6D_6. For example, reaction of **Mo**N_2 with ~3 equiv of NH_3 under an argon atmosphere yields a mixture of **Mo**(NH_3) and **Mo**N_2 that contains 98% **Mo**(NH_3); this mixture is unchanged over a period of 6 months. The ^{1}H NMR spectrum of **Mo**(NH_3) is strikingly similar to that of **Mo**N_2, although the characteristic resonances of **Mo**(NH_3) are distinctly shifted and broadened relative to those of **Mo**N_2.

It proved possible to measure the equilibrium constant for the reaction shown in eq 12 by employing **Mo**($^{15}NH_3$) and **Mo**($^{15}N_2$). Treatment of **Mo**($^{15}NH_3$)$^+$ with 2 equiv of $CrCp^*_2$ in C_6D_6 under an atmosphere of $^{15}N_2$ afforded an equilibrium mixture of **Mo**($^{15}NH_3$), $^{15}N_2$, **Mo**($^{15}N_2$), and $^{15}NH_3$. The concentrations of **Mo**($^{15}NH_3$) and **Mo**($^{15}N_2$) could be determined by proton NMR

$$\mathbf{Mo}(NH_3) + N_2 \rightleftarrows \mathbf{Mo}(N_2) + NH_3 \qquad (12)$$

$$K_{12} = \frac{[\mathbf{Mo}N_2][NH_3]}{[\mathbf{Mo}(NH_3)][N_2]}$$

while the ratio of dissolved $^{15}NH_3$ to $^{15}N_2$ could be determined by ^{15}N NMR, all at 50 °C (Figure 5). The resonance for dissolved $^{15}NH_3$ was too broad at 22 °C to obtain a reliable integral, presumably as a consequence of exchange of free ammonia with bound ammonia in paramagnetic **Mo**($^{15}NH_3$). Increasing the temperature to 50 °C resulted in sharpening of the resonances for **Mo**($^{15}NH_3$) in the ^{1}H NMR spectrum and $^{15}NH_3$ in the ^{15}N NMR spectrum and the amount of $^{15}NH_3$ in solution therefore could be recorded over a period of 14 h. The value of K_{12}(^{15}N, 50 °C) so obtained was found to be 1.16(6). Since the equilibrium shown in eq 12 is likely to have a small $\Delta S°$, and neglecting any $^{15}N/^{14}N$ equilibrium isotope effects, $\Delta G° \approx \Delta H° = -0.09(3)$ kcal/mol. In short, exchange of dinitrogen for ammonia at **Mo** is essentially thermoneutral.

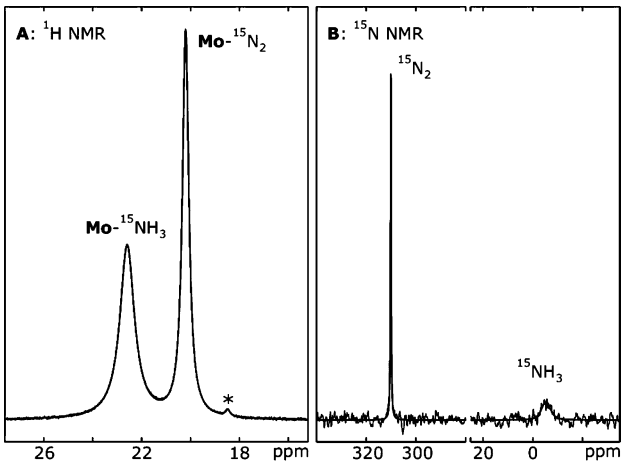

Figure 5. ^{1}H (A) and ^{15}N NMR (B) spectra recorded on an equilibrium mixture of **Mo**($^{15}NH_3$), $^{15}N_2$, **Mo**$^{15}N_2$, and $^{15}NH_3$ at 50 °C in C_6D_6, overlaid with simulated line shapes, and peak assignments. An asterisk in A marks an impurity.

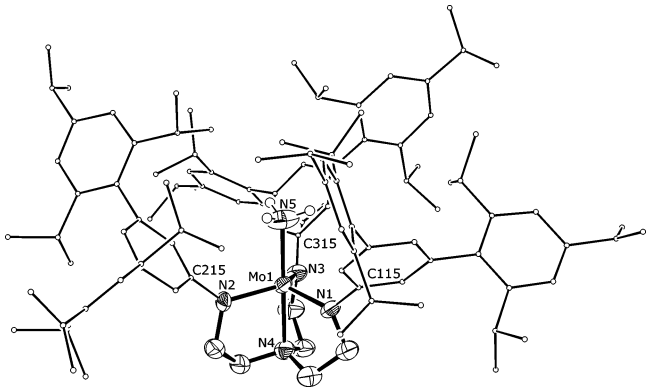

Figure 6. Structure of **Mo**(NH_3) with hydrogens omitted (except N5H_3).

Treatment of a heptane solution of **Mo**N_2 with ~4 equiv of NH_3, followed by storage of the solution for 6 months under 1 atm of argon at room temperature afforded brown crystals of **Mo**(NH_3) that were amenable to an X-ray crystallographic study. The structure of **Mo**(NH_3) was solved and refined (Tables 1 and 2, Figure 6). No evidence of cocrystallization of **Mo**N_2 with **Mo**(NH_3) was found; the ammonia hydrogens were not located. (Although the metric parameters of the $[HIPTN_3N]^{3-}$ ligand are statistically indistinguishable from those in the structure of **Mo**N_2, **Mo**N_2 crystallizes in the space group *C*2/*c* and has a Mo−N5 bond distance 0.2 Å shorter than the Mo−N5 bond distance **Mo**(NH_3).) One-electron reduction of **Mo**(NH_3)$^+$ leads to a slight lengthening of Mo−N_{amide} bond distances (by an average of 0.05 Å), shortening of the Mo←NH_3 bond (by 0.07 Å), and lengthening of the trans Mo−N(amine) bond (by 0.06 Å, Table 2). While these small changes in bond distances in general are consistent with an electron being added to a d_{xz} or d_{yz} orbital on Mo, why the Mo←NH_3 bond shortens upon reduction of **Mo**(NH_3)$^+$ to **Mo**(NH_3) is not clear to us.

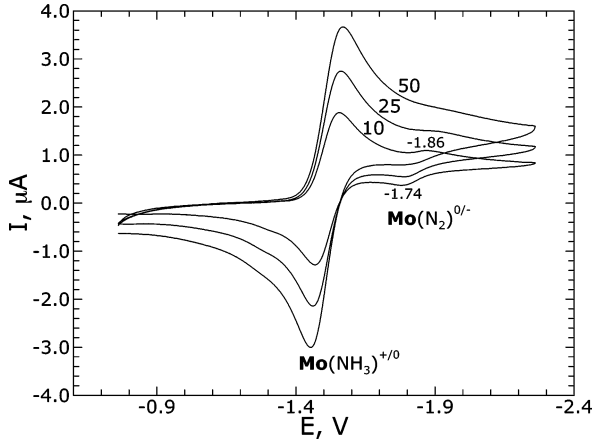

Figure 7. CV of **Mo**$(NH_3)^+$ in THF (0.4 M $[Bu_4N][PF_6]$), showing appearance of **Mo**N_2 at progressively slower scan rates (mV/s).

Electrochemical reduction of **Mo**$(NH_3)^+$ is fully reversible in both THF and PhF (Table 3). Interestingly, at slow scan rates (~10 mV/s), waves corresponding to the **Mo**$N_2^{0/-}$ couple become discernible (near −1.8 V in THF), as shown in Figure 7. Therefore exchange of ammonia in **Mo**(NH_3) with dinitrogen takes place to an observable extent during the course of the experiment. (We plan to measure the rate of conversion of **Mo**(NH_3) into **Mo**(N_2) directly in future studies.) Since the potentials of $CrCp^*_2{}^{+/0}$ and **Mo**$(NH_3)^{+/0}$ in fluorobenzene are identical (both −1.63 V; Table 3), $CrCp^*_2$ is a viable reductant under catalytic conditions, with precipitation of $[CrCp^*_2][BAr'_4]$ providing the extra driving force, as established independently in reactions in C_6D_6 (vide supra).

MoN_2 undergoes a reversible reduction in 0.1 M $[Bu_4N][BAr'_4]$ in PhF at −2.11 V (Table 3, (Figure 8 left), and surprisingly a reversible oxidation at −0.66 V (Figure 8 left). In comparison the oxidation of **Mo**N_2 is irreversible at a platinum disk electrode in THF (Figure 8 right) at the same scan rate. The oxidized species[32,33] is assigned as the product of one-electron oxidation of **Mo**N_2, i.e., 16-electron **Mo**N_2^+. The **Mo**$N_2^{+/0}$ potential in PhF (−0.66 V; Table 3) is nearly 1 V higher than the **Mo**$(NH_3)^{+/0}$ value, i.e., **Mo**$(NH_3)^+$ is more difficult to reduce than **Mo**N_2^+ by ~1V. This substantial difference can be ascribed to the stronger σ-donating properties of ammonia, as well as the fact that the electron added to **Mo**N_2^+ can go into π-bonding orbitals that are largely located on dinitrogen. This potential difference allows us to estimate the free energy of dinitrogen/ammonia exchange at the cationic **Mo**$(IV)^+$ center. As shown in Scheme 4, $\Delta G_{IV}^\circ = \Delta G_{III}^\circ + F(E^{\circ\prime}(\mathbf{Mo}N_2^{+/0}) - E^{\circ\prime}(\mathbf{Mo}(NH_3)^{+/0})) \approx +22$ kcal/mol. The activation energy for unimolecular conversion of **Mo**$(NH_3)^+$ into **Mo**$(N_2)^+$ therefore must be at least 22 kcal/mol, and probably significantly more. Therefore conversion of **Mo**$(NH_3)^+$ into **Mo**$(N_2)^+$ would appear to be slower by at least an order of magnitude than the conversion of **Mo**(NH_3) into **Mo**(N_2). At least we can say that conversion of **Mo**$(NH_3)^+$ into **Mo**(NH_3) facilitates the exchange of ammonia for dinitrogen, which is what one would conclude simply upon considering bonding of ammonia versus dinitrogen to a positively charged Mo(IV) center versus a neutral Mo(III) center. Therefore reduction of **Mo**$(NH_3)^+$ to **Mo**(NH_3) would appear to be imperative for *efficient* formation of **Mo**(N_2).

Scheme 4. Estimate of the Free Energy of Dinitrogen/Ammonia Exchange at the $Mo(IV)^+$ Center

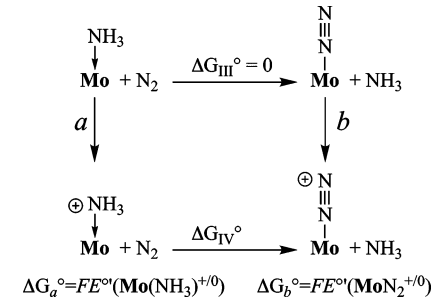

Although the role of **Mo**(NH_3) in the catalytic cycle appears to be mostly that of a precursor to **Mo**N_2, **Mo**(NH_3) may also act as a reductant, since its redox potential is the lowest of all we have measured except that for the **Mo**$N_2^{0/-}$ (Table 3). Under catalytic conditions, **Mo**(NH_3) may effectively store electrons from $CrCp^*_2$. In accord with this proposal, treatment of **Mo**(NH_3) (generated by reduction of

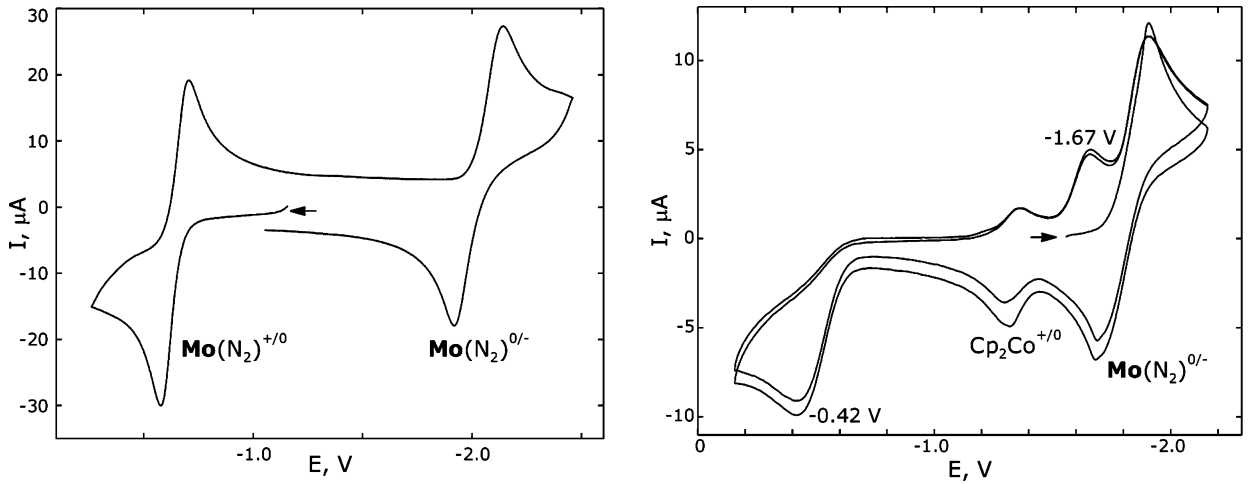

Figure 8. Electrochemical behavior of **Mo**N_2 in 0.1 M $[Bu_4N][BAr'_4]$PhF (left), recorded at a glassy carbon electrode (3 mm dia) at 0.5 V/s and in 0.4 M $[Bu_4N][PF_6]$ THF (right), recorded at a platinum disk electrode (1.6 mm dia) at 0.5 V/s. Initial directions of scans are shown with arrows. The potential scale is referenced to $FeCp_2^{+/0}$.

Mo$(NH_3)^+$ with ~0.9 equiv of $CrCp^*_2$ under dinitrogen) with 1.2 equiv of [2,6-LutH][BAr'_4] resulted in instantaneous formation of **Mo**$(NH_3)^+$ as the sole observable **Mo** species. This result is consistent with **Mo**(NH_3) acting as a reductant toward the small amount of **Mo**N_2 that is formed when ammonia exchanges with N_2.

$$\mathbf{Mo}(NH_3) + {}^1/_6N_2 + 1H^+ \rightarrow \mathbf{Mo}(NH_3)^+ + {}^1/_3NH_3 \quad (13)$$

Therefore **Mo**(NH_3) can be converted into **Mo**$(NH_3)^+$ as shown in eq 13. One-sixth of the **Mo**(NH_3) is converted into **Mo**(N_2); the remaining five-sixths, together with 1 equiv of acid, effects the five-electron, six-proton reduction (per Mo) to give **Mo**$(NH_3)^+$. Since ^{1}H NMR analysis of the reaction mixture at the end of a catalytic run showed all active **Mo** to be present as **Mo**$(NH_3)^+$, the reaction shown in eq 13 may even represent the steady-state stoichiometry of the catalytic system, i.e., **Mo**$(NH_3)^+$ is the resting state. Upon reduction of **Mo**$(NH_3)^+$ by $CrCp^*_2$, **Mo**(NH_3) both binds dinitrogen to give $^1/_6$ equiv of **Mo**(N_2) and supplies $^5/_6$ electrons to yield $^5/_6$ equiv of **Mo**$(NH_3)^+$ and $^1/_3$ equiv of ammonia.

MoH, Its Potential Relevance to Dinitrogen Reduction, and Isolation of a 2,6-Lutidine Adduct. The hydride **Mo**H was initially identified as the major product of the acid-catalyzed (Et_3NH^+) decomposition of **Mo**N═NH and isolated from that reaction in 62% yield.[19] Since then, it has been observed frequently in reaction mixtures in which dinitrogen has been partially reduced. For example, **Mo**N═NH, formed through reduction of **Mo**═NNH_2^+ with $CrCp^*_2$ or $CoCp^*_2$ (vide supra), decays to negligible levels after 24 h in the presence of excess reductant to yield predominantly **Mo**H. It also would seem possible for ammonia to dissociate from **Mo**(NH_3) and for **Mo** to then be protonated to give **Mo**H^+ (in competition with binding of dinitrogen), which subsequently would be reduced to **Mo**H. Although we initially considered the possibility that **Mo**H would be an unreactive thermodynamic sink in catalytic reactions, catalytic runs in which **Mo**H is the "precatalyst" reveal that it is in fact as competent (65−66% efficiency in electrons) as any other molybdenum species that we have used.[20] Therefore, mechanistic investigations as to how **Mo**H is related to the intermediates of dinitrogen reduction are of interest. A more convenient, one pot synthesis of **Mo**H directly from **Mo**Cl is shown in eq 14. [**Mo**(NH_3)][BPh_4] need not be isolated, but can be treated with the hydride reagent immediately.

$$\mathbf{Mo}Cl \xrightarrow[1.1NaBPh_4]{4NH_3} [\mathbf{Mo}(NH_3)][BPh_4] \xrightarrow[1\ M\ THF]{LiBHEt_3} \mathbf{Mo}H \quad (14)$$

Exposure of a C_6D_6 solution of **Mo**H to 1 atm of H_2 resulted in formation of a mixture of **Mo**H and ~20% of a diamagnetic product. This process is reversed upon removal of hydrogen. Although the precise nature of this diamagnetic product is not yet known we believe it is likely to have the stoichiometry "**Mo**H_3". It should be noted that classical

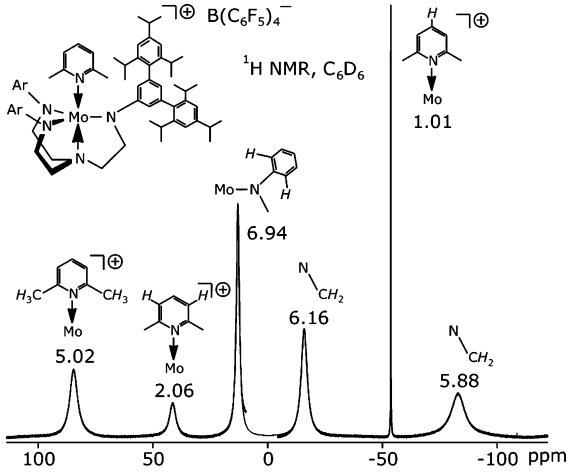

Figure 9. Paramagnetic region of the 500 MHz ^{1}H NMR spectrum of [**Mo**(2,6-Lut)][$B(C_6F_5)_4$] in C_6D_6, overlaid with simulated line shape, with peak assignments and relative integral values.

tungsten trihydride species, [RN_3N]WH_3, have been identified in which R = Me_3Si[34] or HIPT,[35] and that [$HIPTN_3N$]-WH_3 will lose H_2 when heated in vacuo to form mixtures of [$HIPTN_3N$]WH_3 and [$HIPTN_3N$]WH.[36] Exposure of a solution of **Mo**H to D_2 led to formation of an observable quantity of HD after 50 min (according to proton NMR spectra) and yielded largely **Mo**D after 23 h, as determined by IR, consistent with reversible formation of **Mo**H_3.

A slow reaction between **Mo**H and [2,6-LutH][BAr'_4] in C_6D_6 results in complete conversion of **Mo**H into a single paramagnetic **Mo** derivative and free H_2 over a period of 18 h at 22 °C. The ^{1}H NMR spectrum of the final product features several paramagnetically shifted resonances, in addition to resonances characteristic of a high-spin Mo(IV) environment, and whose integrated intensities are consistent with 2,6-lutidine in the coordination sphere of cationic **Mo**$(IV)^+$ (Figure 9). Use of [2,6-LutH][$B(C_6F_5)_4$] in an analogous reaction with **Mo**H (eq 15) afforded a product whose cation had an identical ^{1}H NMR spectrum to that obtained using [2,6-LutH][BAr'_4] (Figure 9), although the [$B(C_6F_5)_4$]$^-$ salt is considerably less soluble than the $BAr'_4{}^-$ salt and could be isolated more readily.

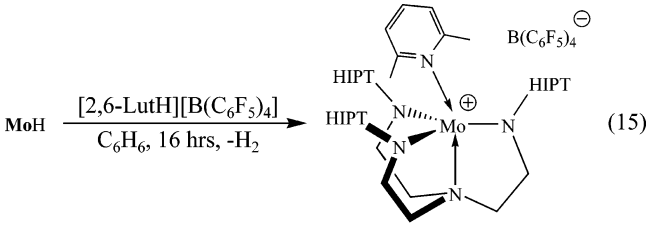

[**Mo**(2,6-Lut)][$B(C_6F_5)_4$], 75%

An X-ray crystallographic study of [**Mo**(2,6-Lut)][$B(C_6F_5)_4$] (Tables 1 and 2, Figure 10) confirmed that it is a 2,6-lutidine adduct of **Mo**$^+$. In [**Mo**(2,6-Lut)][$B(C_6F_5)_4$] the 2,6-lutidine is coordinated to the molybdenum center via the nitrogen

(32) Gassman, P. G.; Sowa, J. R., Jr.; Hill, M. G.; Mann, K. R. *Organometallics* **1995**, *14*, 4879.
(33) Ohrenberg, C.; Geiger, W. E. *Inorg. Chem.* **2000**, *39*, 2948.
(34) Dobbs, D. A.; Schrock, R. R.; Davis, W. M. *Inorg. Chim. Acta* **1997**, *263*, 171.
(35) Yandulov, D. Unpublished results.
(36) Yandulov, D. V.; Schrock, R. R. *Can. J. Chem.*, in press.

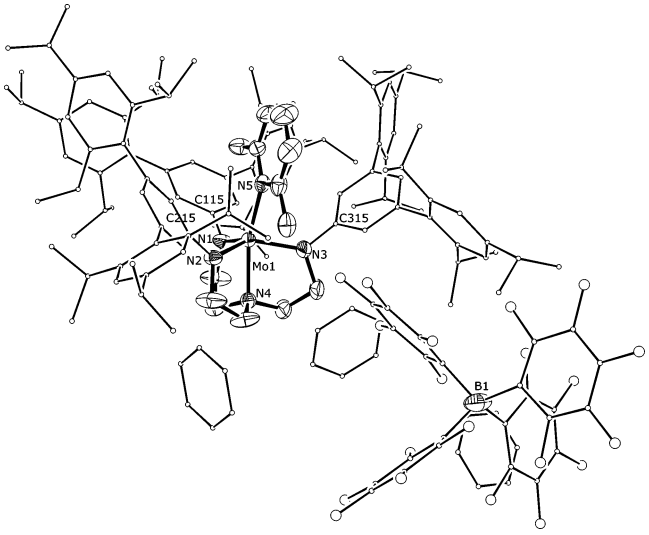

Figure 10. Structure of [**Mo**(2,6-Lut)][$B(C_6F_5)_4$] along with three molecules of benzene of crystallization (hydrogens omitted).

donor with the Mo←N5 distance being 2.283(4) Å, which is within the range of Mo←N(amine) dative bond distances observed in nine other **Mo** structures that we have examined. The 2,6-lutidine is wedged between two HIPT substituents and lies nearly in the plane formed by N1, Mo, and N4 (the interplanar angle Pyr/N4−Mo−N1 is 8°). 2,6-Lutidine is accommodated in the sterically congested **Mo**$^+$ site with surprisingly modest distortions of the $[HIPTN_3N]^{3-}$ ligand framework. The N5−Mo1−N4 angle is only 157.03(14)° with the lutidine bent away from N1, and the N2−Mo−N3 angle opened by ∼10° from the average value found in related structures (115−120°). The 2,6-lutidine itself is virtually undistorted. In order to accommodate an ortho methyl group in the 2,6-lutidine even in this "bent" manner, the HIPT substituent on N1 must adopt a nearly orthogonal relationship (86°) between the plane of the N1 amide and that of the inner aryl ring of the HIPT substituent bound to N1. For comparison, the typical range of such Ar(i)/Mo−N−C−C angles is 24.3−69.3° (Table 2). Aside from this feature, the Mo−N distances and Mo−N(amide)−C(ipso), N(amide)−Mo1−N4, and N4−Mo1−N−C(ipso) angles are typical, although the outer rings of the terphenyl groups are forced into the plane of the inner rings to a slightly greater extent (av Ar(o)/Ar(i) 76.7°) than usual (av >81.9°), as a consequence of the increased overall steric crowding. Although the HIPT substituents of N2 and N3 adopt orientations that are distinct and quite different (the twist angles Ar(i)/Mo−N−C−C are 36°(N2) and 59°(N3)), the very approximate overall C_s symmetry is apparently sufficient to accommodate both envelope conformations of the N(amide)−Mo−N4−C−C rings equally well; the two, opposite gauche conformations around the Mo←N4 bond, were refined as a well-behaved 61:39 disordered mixture.

A search of the Cambridge crystallographic database revealed that over 100 2,6-lutidine adducts have been characterized structurally. However, these typically involve transition metal centers that have a relatively low coordination number (e.g., Cu(I)). Coordination of 2,6-lutidine to the crowded **Mo**$^+$ fragment suggests that the highly electrophilic metal center overcomes the steric and electronic limitations of such bonding, and that the $[HIPTN_3N]^{3-}$ ligand framework is relatively flexible. Bending of the N5−Mo−N4 unit from linearity, which is driven by steric repulsion between the inner aryl ring of the HIPT group attached to N1 and the lutidine methyl group pointed toward it, suggests that a $2\sigma,1\pi$ combination of the three frontier orbitals (d_{xz}, d_{yz}, d_{z^2}) is being employed, much as is found in the cyclopentylidene hydride complex, $[Me_3SiN_3N]W(C_5H_8)H$, in which the N_{amine}−W═C angle is 150°.[37,38] Although exchange between bound and free 2,6-lutidine in solution is not evident in terms of ^{1}H NMR line broadening, $[HIPTN_3N]^{3-}$ ligand resonances are consistent with effective C_{3v} symmetry. We propose that the resonances for 2,6-lutidine are averaged on the NMR time scale as a consequence of an effective rotation of the bound 2,6-lutidine about the N4−Mo axis in concert with a rocking motion within the coordination cavity.

Little is known at this stage about the intermediate in the reaction shown in eq 15. Perhaps the most likely possibility is that this intermediate is **Mo**$(H_2)^+$ (either a dihydride or a dihydrogen complex), and that some time is required for **Mo**$(H_2)^+$ to lose hydrogen and form [**Mo**(2,6-Lut)]$^+$ in the presence of 2,6-lutidine. Since the reaction between **Mo**H and [2,6-LutH][BAr′$_4$] in the presence of 10 equiv of 2,6-lutidine resulted in only 50% conversion of **Mo**H to [**Mo**(2,6-Lut)]$^+$ after 10 days, formation of **Mo**$(H_2)^+$ is likely to be a readily reversible equilibrium, and the formation of [**Mo**(2,6-Lut)]$^+$ slow in part for that reason. We know that **Mo**N_2 reacts with 1 atm of H_2 to yield an unidentified paramagnetic species, "**Mo**(H_2)," which reverts to **Mo**N_2 when the hydrogen atmosphere is replaced with N_2, fully and on the time scale similar to that of exchange of NH_3 for dinitrogen. Therefore, if **Mo**$(H_2)^+$ were to be reduced to **Mo**(H_2) under catalytic conditions, **Mo**N_2 and dihydrogen would form readily. We also know that reduction of **Mo**(2,6-Lut)$^+$ with $CrCp^*_2$ in C_6D_6 under N_2 affords **Mo**N_2 and free 2,6-lutidine upon mixing (eq 16). Presumably **Mo**(2,6-Lut) readily loses 2,6-lutidine from the neutral d^3 center to yield **Mo**, and **Mo** binds dinitrogen to yield **Mo**N_2.

$$\mathbf{Mo}(2,6\text{-Lut})^+ + CrCp^*_2 + N_2 \rightarrow \mathbf{Mo}(N_2) + CrCp^*_2{}^+ + 2,6\text{-Lut} \quad (16)$$

Taken together these data suggest that (i) under catalytic conditions dihydrogen could form via protonation of any **Mo**H that is present to give **Mo**$(H_2)^+$, which is then reduced to yield **Mo**N_2 and dihydrogen, and that (ii) the 2,6-lutidine that builds up during a catalytic reaction is not likely to inhibit formation of **Mo**N_2 by binding to **Mo** to yield **Mo**(2,6-Lut). Although dihydrogen can form at the metal through a hydrogenase-like reaction in catalytic dinitrogen reductions, it seems more likely to us that most dihydrogen is formed primarily by direct reaction of the acid with the relatively

(37) Schrock, R. R.; Seidel, S. W.; Mösch-Zanetti, N. C.; Dobbs, D. A.; Shih, K.-Y.; Davis, W. M. *Organometallics* **1997**, *16*, 5195.
(38) Schrock, R. R.; Shih, K.-Y.; Dobbs, D.; Davis, W. M. *J. Am. Chem. Soc.* **1995**, *117*, 6609.

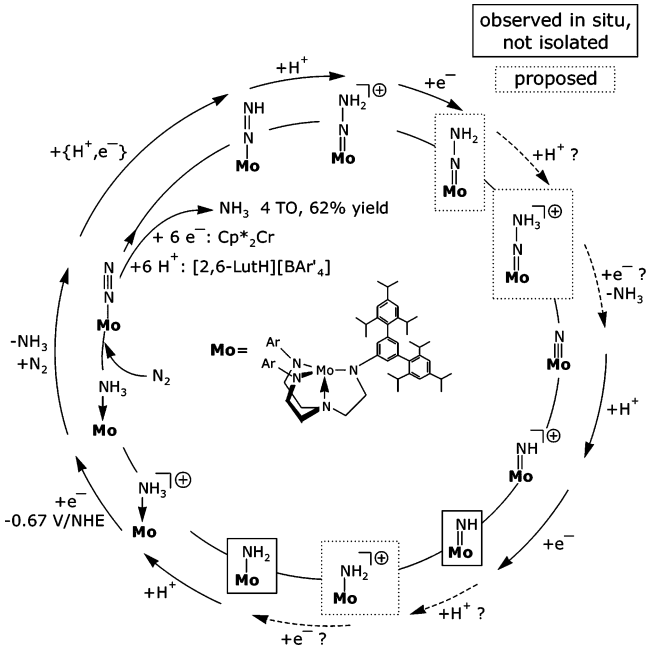

Figure 11. A sequence of elementary steps comprising catalytic reduction of dinitrogen to ammonia by **Mo**. Proposed steps are shown with dashed arrows.

strong reducing agent ($CrCp^*_2$). At this stage it is still unknown how much hydrogen is formed. To what extent it is formed by direct reduction of the acid by the reducing agent versus "hydrogenase" activity may be indeterminate.

Summary and Comments

Figure 11 shows the proposed mechanism of catalytic reduction of dinitrogen to ammonia at **Mo**. Seven of the proposed intermediates (eight if **Mo**N_2^- is included) have been isolated and structurally characterized, and two more have been generated in situ and identified spectroscopically. One-electron, one-proton reduction of **Mo**N_2 to **Mo**N═NH could proceed by any of the three mechanisms shown in Scheme 2; none can be ruled out at this stage. **Mo**N═NH is protonated by [2,6-LutH][BAr′$_4$] in C_6D_6 to yield an equilibrium mixture of **Mo**N═NH and **Mo**═NNH_2^+. Reductions of isolated **Mo**═NNH_2^+ with all metallocene reductants examined (Table 4) proceed to completion rapidly at 22 °C, but "**Mo**═NNH_2" cannot be observed. Instead, only products of its disproportionation are observed, including **Mo**≡N and ammonia that are proposed to form via protonation of "**Mo**═NNH_2" and reduction of the resulting "**Mo**═NNH_3^+" (Scheme 2). **Mo**≡N is protonated with [2,6-LutH][BAr′$_4$] in C_6D_6 to form an equilibrium mixture with **Mo**═NH^+, whose reduction yields a metastable product tentatively assigned as "**Mo**═NH". Despite exhibiting a considerably greater stability than "**Mo**═NNH_2", we have not been able to isolate "**Mo**═NH" in pure form. Decomposition of "**Mo**═NH" in C_6D_6 yields an equimolar mixture of **Mo**≡N and "**Mo**(NH_2)"; **Mo**(NH_2) can be protonated by **Mo**═NH^+ to give **Mo**$(NH_3)^+$, whose deprotonation affords **Mo**(NH_2) independently. The sequence of reactions leading to **Mo**(NH_2) from **Mo**═NH is proposed to consist of protonation of **Mo**═NH followed by reduction of the resulting **Mo**$(NH_2)^+$ (Scheme 3). Like **Mo**═NH, **Mo**(NH_2) is prone to disproportionation and has not yet been isolated in pure form. Reduction of isolated **Mo**$(NH_3)^+$ with $CrCp^*_2$ affords **Mo**(NH_3), which equilibrates with **Mo**N_2 under N_2, but is otherwise stable under an atmosphere of argon for extended periods of time. The dinitrogen/ammonia exchange equilibrium at **Mo**(III) is characterized by $\Delta G° \approx 0$, while exchange at **Mo**$(IV)^+$ has an estimated $\Delta G°$ of greater than +22 kcal/mol. Loss of ammonia from **Mo**(NH_3) under dinitrogen to give **Mo**(N_2) has been shown to proceed to an observable extent in a CV experiment. Finally, if any **Mo**H is formed during a catalytic reaction at least some dihydrogen can be formed through a hydrogenase-like reaction.

All "disproportionations" (of "**Mo**═NNH_2", "**Mo**═NH", and "**Mo**(NH_2)") are proposed to take place via a sequence of electron- and proton-transfer reactions, with the proton transfers being mediated by a base (e.g., traces of free ligand) in C_6D_6 or by 2,6-lutidine under catalytic conditions in heptane. These disproportionations have no adverse effect on dinitrogen reduction. Instead, they illustrate the facility with which extended sequences of proton transfer and electron-transfer reactions involving dinitrogen at various stages of reduction can take place at the **Mo** center. In view of the fact that these disproportionations can be observed it seems unlikely that catalytic dinitrogen reduction proceeds "linearly" through all fourteen intermediates shown in Figure 1.

The accumulated structural data (Table 2) show that the geometry of the auxiliary triamidoamine ligand responds to the stepwise reduction of dinitrogen primarily, and almost exclusively by variation of the Mo←N_{amine} bond distance. As the N−N bond is weakened and ultimately cleaved on going from **Mo**N_2 to **Mo**≡N, the Mo−N_α bond is transformed from a dative to a triple bond. The decrease of Mo−N_α distance by 0.31 Å parallels the increased *trans*-influence of the N_α fragment, which leads to lengthening of the *trans* Mo←N(amine) bond by 0.21 Å. Subsequent reduction of the nitride to bound ammonia lengthens Mo−N_α by 0.52 Å and shortens Mo ← N(amine) by 0.19 Å. Throughout this profound transformation that spans four Mo oxidation states, the average Mo−N_{amide} distances vary by only 0.09 Å, the average N_α−Mo−N_{amide} and Mo−N_{amide}−C_{ipso} angles remain within 4° and 5° of each other, respectively, while N_α−Mo−N_{amide}−C_{ipso} dihedral angles stay at under 12.6° for all structures except for **Mo**$(NH_3)^+$, which has one anomalous value of 19.5°. The aryl rings of the terphenyl moieties remain essentially orthogonal (average angles between mean-square planes of inner and outer rings vary from 83.6° to 86.8°). Last, terphenyl substituents are found to adopt two distinct orientations with respect to the mean-square planes of the amide nitrogens, with interplanar angles being either ∼30° or ∼60° without any apparent preference. The lack of a pronounced structural variation of the **Mo** fragment that accompanies six-electron reduction of dinitrogen is clearly beneficial to the facility of the catalytic process, as dinitrogen reduction therefore can proceed with minimal reorganization of the ligand framework.

We are in the process of studying variations of the catalytic dinitrogen reduction in depth. Some of the most important variations will be altered sterics in the ligand, solvent effects, the acid source (including the anion), and pressure and temperature effects. We also want to quantify dihydrogen, study the kinetics of conversion of **Mo**(NH_3) into **Mo**(N_2), and carry out inhibition studies (e.g., by dihydrogen or ammonia). We are also exploring chemistry of **Mo**L species in which the ligands L (e.g., acetylene, isonitriles, and azide) are also substrates for FeMo nitrogenase. Finally, we are exploring the possibility of extending to V the principles we have learned for Mo, where a dianionic ligand may be required in order to produce intermediates similar to those shown in Figure 1 in which vanadium will be in an oxidation state of 2+, 3+, 4+, or 5+.

Experimental Section

General. All manipulations of air- and moisture-sensitive compounds were carried out by standard Schlenk and glovebox techniques under an atmosphere of nitrogen using flame- and oven-dried glassware, including NMR tubes. Ether, pentane, and toluene were purged with nitrogen, passed through activated alumina columns,[39] and freeze−pump−thaw degassed three times; THF, DME, 1,4-dioxane, and benzene were distilled from dark purple Na/benzophenone ketyl solutions; CH_2Cl_2 and MeCN were distilled from CaH_2; PhF was distilled from P_2O_5 under N_2; all dried and deoxygenated solvents were stored over molecular sieves in a nitrogen-filled glovebox. Small quantities of regular hydrocarbon and ether solvents, as well as all such deuterated NMR solvents were additionally purified by vacuum transfer from dark-purple solutions/suspensions of Na/benzophenone ketyl (CaH_2 for CH_2Cl_2, PhF and CD_2Cl_2), degassed, and stored in gastight solvent bulbs inside a glovebox. The reagents $CoCp_2$ (sublimed), $CrCp^*_2$, $[CoCp^*_2][PF_6]$, $NaBPh_4$ (ground and dried in vacuo at 110 °C) (Strem), $LiBHEt_3$ (1 M THF) (Aldrich) were used as received, unless indicated otherwise. Potassium graphite (KC_8) was prepared by stirring freshly cut potassium metal and graphite in 1:8 stoichiometry with a glass-coated stirbar under 700 Torr of Ar at 140 °C for an hour. $CoCp^*_2$ was prepared from $[CoCp^*_2][PF_6]$ and a slight excess of KC_8 in THF over 4 h at 22 °C and sublimed. [2,6-LutH][$B(C_6F_5)_4$] was prepared from $[Ph_3C][B(C_6F_5)_4]$ and 2,6-LutHCl in CH_2Cl_2. All **Mo** compounds mentioned in the text were prepared as described in the literature or as described below. All metal complexes were stored in the dark, under N_2 at −35 °C. ^{1}H, ^{19}F, and ^{15}N NMR spectra were recorded on a Varian Mercury 300 (^{1}H, 300 MHz; ^{19}F, 282 MHz) or a Varian Inova 500 (^{1}H, 500; ^{15}N, 50.7 MHz) spectrometers and referenced to the residual protio solvent peaks (^{1}H) or external neat PhF (^{19}F, −113.15 ppm relative to $CFCl_3$) and neat MeCN (^{15}N, +245.5 ppm relative to neat NH_3) at 303 K.[40] Ammonia was determined uing the indophenol method.[41,42] Elemental analyses were performed by H. Kolbe Mikroanalytisches Laboratorium, Mülheim an der Ruhr, Germany.

Electrochemical measurements were carried out using BAS CV-50W potentiostat, 0.4 M $[Bu_4N][PF_6]$/THF, or 0.1 M $[Bu_4N][BAr'_4]$/PhF electrolytes, and a standard three-electrode cell assembly with platinum (1.6 mm dia) or glassy carbon (3.0 mm dia) disk working electrodes, platinum wire auxiliary electrode, and reference electrodes consisting of either a silver wire submerged in a 10 mM solution of AgOTf in 0.4 M $[Bu_4N][PF_6]$/THF electrolyte or a AgCl-coated silver wire submerged in 0.1 M $[Bu_4N][BAr'_4]$/PhF electrolyte. All measurements were referenced externally and/or internally with $FeCp_2$, $CoCp_2$ or **Mo**N_2, as appropriate.

Generation of [HIPTN$_3$N]Mo(NH$_3$). Ammonia (∼4 equiv) was vacuum-transferred to a frozen C_6D_6 solution of **Mo**N_2 that had been freeze−pump−thaw degassed five times in an NMR tube fitted with a Teflon valve. The solution was thawed and exposed to 1 atm of argon. Periodic monitoring of the solution contents by ^{1}H NMR showed formation of the title product in >95% purity after 16 h at RT, which remained unchanged after additional 6 months: ^{1}H NMR (C_6D_6, 20 °C) δ 26.6 (s, 6H, NCH_2), 7.27 (s, 12H, 3,5,3″,5″-*H*), 4.32 (s, 3H, 2′-*H*), 3.07 (br septet, J_{HH} = 6 Hz, 6H, 4,4"-C*H*Me$_2$), 1.80 (br s, 36H, 2,6,2″,6″-CH(CH_3)$_2$), 1.10 (d, J_{HH} = 6.6 Hz, 36H, 4,4″-CH(CH_3)$_2$), 0.98 (s, 36 H, 2,6,2″,6″-CH-(CH_3)$_2$), −0.07 (br s, 12H, 2,6,2″,6″-C*H*Me$_2$), −0.61 (br s, 6H, 4′,6′-*H*), −27.9 (s, 6H, NCH_2).

X-ray quality crystals were obtained over a six-month period at 22 °C from a solution of **Mo**N_2 (70 mg) in heptane that had been treated with ∼4 equiv of NH_3 under 1 atm of argon for 3 days, followed by concentration to ∼0.5 mL and replacement of the atmosphere with fresh argon, all in a Schlenk tube fitted with a Teflon valve.

Measurement of the Equilibrium Constant of Dinitrogen/Ammonia Exchange at Mo(III). Benzene-d_6 (0.8 mL) was freeze−pump−thaw degassed five times and vacuum-transferred to a mixture of solid [**Mo**($^{15}NH_3$)][BAr'_4] (30 mg) and 2 equiv of $CrCp^*_2$, placed in an NMR tube fitted with a Teflon valve. The resulting mixture was thawed and pressurized to 1 atm with $^{15}N_2$, purified by passage through a small column of solid Na/Ph_2CO.[14] The precipitate of $[CrCp^*_2][BAr'_4]$ was centrifuged to the top of the NMR tube prior to the NMR measurements. The ^{15}N NMR spectrum in Figure 5 was acquired with the recycling time (at+d1) set equal to 5 times the T_1 estimated for the resonance of dissolved $^{15}N_2$. The integral ratios of the spectra in Figure 5 were obtained by fitting the experimental data, processed with appropriate line-broadening, with Lorentzian line shapes and the functions necessary to describe any baseline curvature, in the least squares sense using Matlab 6.5 (1984−2003 The MathWorks, Inc., Natick, MA). Specifically, the ^{15}N ammonia peak was fit as a binomial quartet with $^1J(^{15}N-H)$ = 61 Hz, determined from the spectra of pure $^{15}NH_3$ dissolved in C_6D_6.

An Improved Synthesis of [HIPTN$_3$N]MoH. Ammonia (57 mL, 380 Torr, ∼1.16 mmol) was vacuum-transferred from a bronze-colored Na solution to a frozen mixture of **Mo**Cl (500 mg, 0.291 mmol) and $NaBPh_4$ (109.6 mg, 0.320 mmol) in fluorobenzene (10 mL). The resulting mixture was thawed, stirred at 22 °C for 2 h, and filtered through Celite. The filtrate was treated with $LiBHEt_3$ (1 M THF, 291 μL, 0.291 mmol), and the resulting solution was stirred for 15 min and brought to dryness in vacuo. The resulting solid was dried at 75 °C in vacuo and extracted with benzene. The benzene extracts were filtered through Celite and taken to dryness in vacuo. Trituration in pentane (10 mL) afforded a red microcrystalline solid, which was collected by filtration on a frit after standing at −35 °C for several days, washed with cold pentane, and dried in vacuo at 45 °C; yield 326 mg (194 mmol, 67%). This material is identical to that reported previously.

{[HIPTN$_3$N]Mo(2,6-Lut)}[B(C$_6$F$_5$)$_4$]. A mixture of [HIPTN$_3$N]-MoH (58 mg, 34.5 μmol) and [2,6-LutH][$B(C_6F_5)_4$] (28.5 mg, 36.2 μmol) in benzene (1 mL) was stirred for 84 h at room temperature and brought to dryness in vacuo. The residue was extracted with

(39) Pangborn, A. B.; Giardello, M. A.; Grubbs, R. H.; Rosen, R. K.; Timmers, F. J. *Organometallics* **1996**, *15*, 1518.
(40) Witanowski, M.; Stefaniak, L.; Szymanski, S.; Januszewski, H. *J. Magn. Reson.* **1977**, *28*, 217.
(41) Chaney, A. L.; Marbach, E. P. *Clin. Chem.* **1962**, *8*, 130.
(42) Weatherburn, M. W. *Anal. Chem.* **1967**, *39*, 971.

benzene, and the extracts were filtered through Celite and brought to dryness in vacuo. Addition of pentane to the amorphous residue led to formation of a brown-red microcrystalline solid, which was collected by filtration on a frit after standing at −35 °C for several days, washed with cold pentane, and dried in vacuo at 70 °C; yield 63.4 mg (25.7 μmol, 75%): ^{1}H NMR (C_6D_6, 20 °C) δ 84.5 (s, 6H, C_5H_3N-2,6-(C*H*$_3$)$_2$), 41.5 (s, 2H, 2,6-Lut-3-*H*), 13.0 (s, 6H, 4′,6′-*H*), 7.37 (s, 12H, 3,5,3″,5″-*H*), 3.05 (br septet, J_{HH} = 6 Hz, 6H, 4,4″-C*H*Me$_2$), 2.66 (br s, 12H, 2,6,2″,6″-C*H*Me$_2$), 1.45 (d, J_{HH} = 6.0 Hz, 36H, 4,4"-CH(C*H*$_3$)$_2$), 1.10 (br s, 72H, 2,6,2″,6″-CH(C*H*$_3$)$_2$), −15.9 (s, 6H, NC*H*$_2$), −53.66 (s, 1H, −50.1, 2,6-Lut-4-*H*), −82.9 (s, 6H, NC*H*$_2$); the 2′-*H* resonance is obscured; ^{19}F NMR (C_6D_6, 20 °C) δ −130.46 (s, 8F, C_6F_5-2-*F*), −161.94 (s, 4F, C_6F_5-3-*F*), −165.28 (s, 8F, C_6F_5-4-*F*). Anal. Calcd for $C_{145}H_{168}BF_{20}MoN_5$: C, 70.58; H, 6.86; N, 2.84. Found: C, 70.37; H, 7.01; N, 2.74.

X-ray quality crystals were grown from a mixture of benzene and heptane solution at 22 °C. ^{1}H NMR integrals (Figure 9) were obtained from a fitted spectrum, as in the case of **Mo**(NH_3)/**Mo**N_2.

X-ray Crystallography. X-ray data were collected on a Bruker diffractometer equipped with an Apex CCD area detector and a Mo Kα X-ray source. All structures were solved and refined using Bruker SHELXTL 5.1. Carbon density from solvent(s) of crystallization was included in the formulas and refinements as far as possible. Crystals of **Mo**N═NH, **Mo**N═NH_2^+, and **Mo**═NH^+ were grown from a supersaturated pentane solution at 22 °C.

Acknowledgment. R.R.S. is grateful to the National Institutes of Health (GM 31978) for research support, and both R.R.S. and D.V.Y. are grateful to William E. Geiger for advice on practical aspects of electrochemistry in weakly polar media, and to Dr. Peter Mueller and Adam Hock for assistance in X-ray studies.

Supporting Information Available: Crystal data and structure refinement, atomic coordinates and equivalent isotropic displacement parameters, bond lengths and angles, and anisotropic displacement parameters for all crystallographically characterized compounds. This material is available free of charge via the Internet at http://pubs.acs.org.

IC040095W